Granit Mahmuti

Hardware Implementation and Verification of a 10 Gbps Transceiver for Optical Wireless Communication at 1550 nm

MASTERARBEIT

zur Erlangung des akademischen Grades

Diplom-Ingenieur

Masterstudium Elektrotechnik

eingereicht an der

Technischen Universität Graz

Betreuer

Ao. Univ.-Prof. Dipl.-Ing. Dr.techn. Erich Leitgeb

Institut für Hochfrequenztechnik

Graz, September 2020

STATUTORY DECLARATION

I declare that I have authored this thesis independently, that I have not used other than the declared sources / resources, and that I have explicitly marked all material which has been quoted either literally or by content from the used sources.

Date

Signature

Zusammenfassung

Ziel dieser Masterarbeit ist die Entwicklung und der Aufbau eines optischen Transceiver für Freiraumübertragungssysteme für 1550 nm mit eine Datenübertragung bis zu 10 Gbps. Der erste Teil dieser Arbeit besteht darin den theoretischen Hintergrund und die Entwicklung der optischen Freiraumübertragungssysteme zu beschreiben, sowie die Funktionsprinzipien zu erklären. Des Weiteren wird auf das Design eines optischen Systems eingegangen und eine Beschreibung der einzelnen Komponenten erfolgt. Auch die verschiedenen Modulationsarten sowie auch das Funktionsprinzip des optischen Empfängers und Senders werden dargestellt. Dazu werden die Lasersicherheitsklassen und Standards abgebildet, sowie eine detaillierte Analyse des Link Budget.

Der praktische Teil dieser Arbeit widmet sich der Entwicklung des optischen Systems. Daraufhin folgen Messungen und Testungen, die die Funktionalität des Links überprüfen sollte. Das letzte Kapitel enthält abschließende Bemerkungen und die Testungen zeigen, dass das Design des optischen Systems, auch bei einer höheren Datenrate als 10 Gbps, einwandfrei funktioniert. Die Ergebnisse haben gezeigt, dass die Hardware in ein FSO-System integriert werden kann und für weitere Forschungen herangezogen werden kann.

Abstract

The aim of this master thesis is the development and analysis of an optical transceiver for Optical Wireless Communication (OWC) at 1550 nm with a data rate up to 10 Gbps. The first part is to describe the background of Free Space Optical Communication (FSO) systems, their historical development, as well as the principle of operation. Furthermore, the design of an optical system is presented, and a description of the individual components is given. The same applies to the types of modulation techniques and the operating principles of optical receiver and transmitter. Laser safety classes and standards are presented, as well as a detailed analysis of the optical link budget.

The practical part of this thesis presents the physical implementation of the designed optical system. The performance analysis and results are presented and discussed. Last chapter presents conclusion remarks and the successfulness of the implemented hardware and its ability to work at even higher data rate than 10 Gbps. The results show that the hardware can be integrated into a FSO system and can be used for further projects.

Acknowledgment

This thesis was accomplished under the supervision of Leitgeb, Erich, Ao.Univ.-Prof. Dipl.-Ing. Dr.techn in the Institute of Microwave and Photonic Engineering of Graz University of Technology.

First of all, I would like to thank the one person without whose support I would not be able to finish this thesis in such a short time and with such great results. He is not only my best friend at TU Graz but also a great Engineer. Thanks to Ziad for all his support, valuable advices and all the free time he took for me.

I would like to specially thank a wonderful person, Erich who is not only my favorite Professor but also the Supervisor of my thesis and my mentor. He gave me the opportunity to work as a teaching Assistant, where I had the chance to learn many new things and also to work with great people. His valuable advices and support during my studies where very helpful for me and I will always keep a good memory of him.

I would like to thank all my colleges from IKS, IHF and Professor Pommerenke from Electronics Institute. Also, my friend Yingjie that gave me her opinion and support for the final version of my Thesis.

The biggest thanks goes to my biggest support in my life, my parents and my brother. Without their unconditionally love and support it would not be possible to study in Graz and to realize my dream for studying abroad. Thank you for never giving up on me and always believing in me.

And of course a big thank goes to my friend(s) for all the love and support during my studies. Life is much better if you have lovely people around you.

Graz, 2020 Granit Mahmuti

Contents

List of Figures

List of Tables

List of Abbreviations

OWC	Optical Wireless Communication
FSO	Free-Space Optical Communication
FCC	Federal Communications Commission
SNR	Signal to Noise Ratio
BER	Bit Error Ratio
LOS	Line-Of-Sight
MZM	Match-Zehnder Modulator
UV	Ultraviolet
IR	Infrared
LED	Light Emitting Diodes
LD	Laser Diode
IEC	International Electrotechnical Commission
OOK	On-Off Keying
RZ	Return to Zero
NRZ	Non-Return to Zero
IM	Intensity Modulation
DD	Direct Detection
IP	Internet-Protocol
FBG	Fiber Bragg Grating
CCD	Charge-Coupled Devices
CID	Charge Injection Device
PMT	Photomultiplier Tubes
QAPD	Quadrant Avalanche Photodiode
PPM	Pulse Position Modulation
LPPM	Single-Pulse Position Modulation
DPPM	DifferentialPulse Position Modulation
MPPM	Multiple-Pulse Position Modulation
LDO	Low-Dropout Regulator
PCB	Printed Circuit Board

1. Introduction

Chapter 1 explains the general concept of FSO Communication systems, its historical development, starting from their humble beginnings in the early years up to the various powerful methods of modern technology. This chapter also explains the motivation of this work and the ideas that make this thesis so interesting.

Chapter 2 introduces FSO systems and shows the concepts of an optical wireless transceiver design, its main components, transmission data, and the principle of operation and many advantages over other technologies. Each component will be explained starting from the concept of a simple FSO link, up to the optical transmitter and its component from optical sources, modulation technique and optical receiver.

Laser safety standards and classification are discussed in chapter 3, highlighting the importance of choosing the right wavelength and all the potential risks to the human body, especially to the eyes.

Chapter 4 introduces the link analysis, including link budget, transmission losses, optical received signal power et cetera. The purpose is to determine if a communication link can support the target data rate, and if so, with what margin. The case studied here is not for terrestrial communication, but for earth and satellite communication. Link budget simulation of the received power signal and SNR using MATLAB software are found also in chapter 4.

Chapter 5 presents the practical part, where the hardware implementation is discussed. The results of the performance analysis, Bit Error Rate (BER), eye diagram, etc. are also presented.

Chapter 6 presents conclusion and remarks on this work and the use of the optical system for future projects.

1.1 History of Free Space Communication

The origin of telecommunication technology used for transferring information data is a very old technique which has its route from the first man's fire signal to today's technology. The possibility to transfer information in a short time was always one of the priority of every telecommunication company, especially nowadays where the technology evolved so much that it is becoming a must for every company to transfer information in a short time with a high capacity [7].

FSO systems are mainly used in the last mile area. It is a Line-Of-Sight (LOS) technology that allows to transfer information in free space. It is classified as optical communication at the speed of the light, as light travels in free space faster than it does through fiber optics. The communication technology has been used from thousands of years from the Greeks and Romans (around 800 BC) who used polished metal plates as mirrors to communicate with each other. The light was reflected on the polished plates, which gave people the idea of communication. The optical telegraph communication based on a chain semaphores was developed by French Naval (Claude Chappe) in 1792. The US military used also the same principle with sunlight-based power devices to communicate in the 1800s. In 1880 was the famous Alexander Graham Bell (considered as the era of OWC), presented his device with the name *Photophone*. It was a transmission in free space, transmitting a sound signal using a beam of light over a length of about 200 m through the atmosphere medium (See Figure) 1.1 [1] [8] [9].

Figure 1.10: *In 1880, Graham Bell transmitted his voice over more than 600 feet (200m), through the air and using the reflected rays of the sun. In 1999, engineers took up the idea of the photophone*
(source: http://www.bell-labs.com/news/1999/february/ 25/presby_lg.jpeg)

Figure 1.1: Photophone from Alexander Graham Bell [1]

Transmitting high data rate for long distance with free space optical communication requires an amount of strong optical beam at the desired wavelength. In 1960 Theodore Maiman invented the ruby laser, one of the first optical lasers which was a huge success

in the optical field of communication. In wireless communication systems semiconductor injection laser diodes are very attractive especially for long distance. FSO has also been researched for deep space application by NASA (National Aeronautics and Space Administration) and ESA (European Space Agency) with their programs such as Mars Laser Communication Demonstration (MLCD) and the Semiconductor Laser Inter-satellite Link Experiment (SILEX) [9]. 2003 was the year of Internet-Protocol (IP) packets for computer internet network. They carried data using IPs that include voice signals. The new research for sending high speed data up to 400 Gbps (Gigabit per second) over a FSO link is not new especially for the next generation of 5G networks [7].

1.2 Motivation

The 5G technology is not only the future of communication but it is already in the present. Especially the optical transmission of data will play a major role in the future. Therefore, my goal is to develop an optical system that consist of an optical receiver and transmitter. With this work I would like to inspire future students to get involved into the word of FSO communication systems. The hardware of my optical transceiver can be integrated into a FSO system that can be used for future projects.

2. Free Space Optical Communications

FSO requires LOS communication between the receiver and transmitter and the use of lasers to provide narrow beam optical connection. Free space means air, outer space, vacuum, where light is propagated in this medium to transmit information. We can classify free space optic as an optical communication at the speed of the light, as light travels through free space faster than it does through fiber optics. FSO provide cable free communication and has a license-free spectrum [8]. The advantages of FSO over other technologies include:

- Higher bandwidth.
- Higher security.
- Invisible and eye safe.
- Unlicensed spectrum.
- Low bit error rates (BER).
- High directivity.
- Quickly and easily deployment.

But there are also FSO disadvantages since the medium of transmission is air. This includes: atmospheric absorption, weather conditions and turbulence, interference from background light sources ect. which limit the performance of the optical link. FSO has several applications like: telecommunication and computer networking, outdoor wireless access, security applications, last-mile access, point-to-point LOS link ect [10] [8].

Free space communication system is based on three basic components: the transmitter, which converts the electric signal (data) into an optical signal, the channel and the receiver, which decodes the optical signal into an electrical signal (data).

Transmitter: The main function is to convert the electrical signal into an optical signal that propagate through the atmosphere to the receiver. The components of a transmitter consist of: MZM, driver circuit for the optical source, collimator or telescope that collimates and direct the light toward the receiver.

Channel: The atmospheric condition in FSO channel has many unpredictable factors like cloud, snow, fog, rain etc. This limits the performance of FSO systems.

Receiver: The main function is to recover the transmitted data from the received

optical signal. Its telescope collects the transmitted power and reduces the background ambient light. The components of a receiver consist of: receiver telescope, optical filter, photodetector, amplifier, demodulator ect [11].

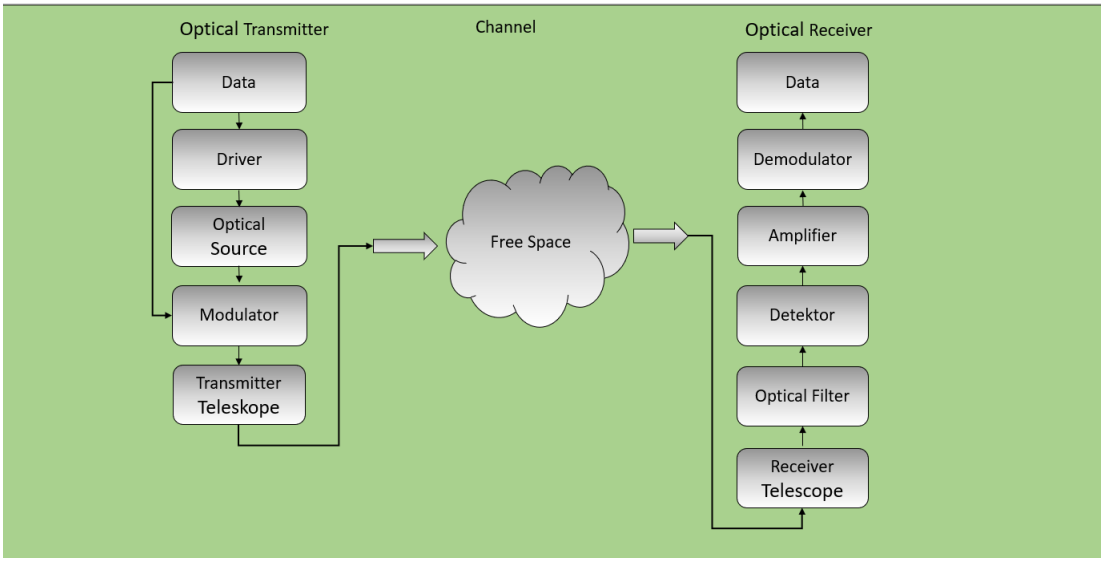

Figure 2.1: Block diagram of FSO communication link

2.1 The Optical Signal

The optical source radiates a planar electromagnetic field. It is described at any time and spatial point by solutions to Maxwell's equations. Plane waves are free-space modes. If we consider a scalar component **U** which is normal in the direction of propagation and ignore the polarization, then the following expression is used

$$U(x, y, z) = A(x, y, t)e^{i(\omega_0 t + \phi(x,y,t))} \tag{2.1}$$

where (x, y) is the plane normal to the direction of propagation, t is time, A is the wave amplitude, ω_0 is the optical radian frequency, ϕ is the phase offset. When optical signal is transmitted, it can be modulated by its amplitude A, frequency $\frac{d\phi}{dt}$ and phase ϕ. $I \sim A^2$ where I is light intensity. If the wave intensity is the only component being detected at the receiver, then we are talking about incoherent systems. On the other hand, coherent systems depend on both the intensity and phase, thus making such systems sensitive to both amplitude and phase changes [12].

2.1.1 Driver Circuit

Driver circuit is very important for optical communication. A driver circuit for a laser diode or other optical sources is to provide precise electrical currents. A constant and

noiseless current is another characteristic that a driver circuit should have in order to emit a stable light signal. For modulators (in this case an MZM) driver circuit should provide a stable biasing current [13].

2.1.2 Optical Source

In optical communication, a device that convert an electrical signal into an optical signal is referred to as an optical source. For optical transmitters and other devices, a suitable light source must have certain characteristics. Choosing the right optical source depends on many factors including optical power, speed, beam profile, high optical output power, low weight and low cost. The two most known optical light sources are: **Light Emitting Diodes (LED)** and **Laser Diode (LD)**.
They offer small size, low forward voltage, drive current ect. LEDs are preferred for indoor application and LD for outdoor application [14].

LED

The LED is a semiconductor light source. It is a forward bias p-n junction that emits light when it is activated. The light is emitted through spontaneous emission. The current flows from p-side to n-side (anode, cathode), but not in reverse direction. Their structure is similar to that of an LD, but it does not have the cavity for feedback. The advantages are: very low voltage from 1-2 Volt, current 5-20 mA, a very long life span, miniature in size, output power less than 150 mW [14] [13].

LD

LASER stands for Light Amplification by Stimulated Emission of Radiation Diode. An LD is a semiconductor p-n junction that emits light coherently. The light is emitted through stimulated emission of electromagnetic radiation. The advantages are: high speed and bandwidth, high efficiency, long lifetime, small in size and very narrow spectral bandwidth duo to its coherent nature, which make it possible to transmit high data rate up to 10Gbps [14] [13].

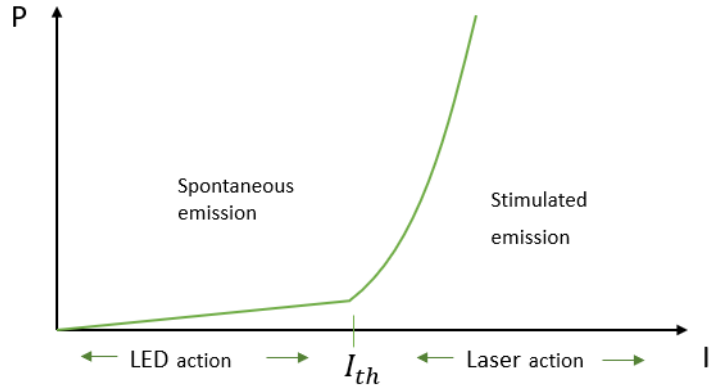

Figure 2.2: Spontaneous and Stimulated emission for LED and LD.
P: Power (W), I: Current (A), I_th: Threshold value.

2.1.3 Modulator

An optical modulator is a device that modulates the light beam and propagate it through free space or optical waveguide. The optical signal parameters are characterized in amplitude, phase, frequency, and polarization [5]. We have two types of modulation methods: **1. Direct Modulation**, where the light source is directly modulated, and **2. External Modulation**, where the light is modulated by an external device, which can produce optical pulses of higher quality and higher bit rates [5]

Direct Modulation

The direct modulation method of the light source (typically laser) is directly modulated, which is the simplest method and has the advantages of simplicity, compactness, and cost effectiveness. On the other side, resulting data rates are limited because of link length and wavelength chirping effects. This creates a bottleneck in the system, which will affect the overall performance [5].

External Modulation

Optical systems use intensity, phase and frequency modulation. The intensity modulation is the most used method, since it simplifies the demodulation at the receiver side with a simple use of a photodiode. In an optical transmitter system, we have two types of external modulators: **The Electroabsorption Modulator (EAM)** and **Mach-Zehnder Modulator (MZM)**. MZM is larger than EAM in size, but it can generate a higher quality of optical pulses, with a controlled amount of superior chirp and a higher Extinction Ratio (ER) characteristics [5].

Mach-Zehnder Modulator

MZM is used to control the phase and the amplitude of the optical signal. Converting the optical phase modulation into an intensity modulation, it is often necessary to use an interferometer. The role of an interferometer is to split the optical waveguide, which comes at the input side, into two different waveguide arms equally. The bias voltage is applied on the splitted waveguides to induce a phase shift, so at the end occurs the effect of interference. At the output we have the converted amplitude-modulated wave. Constructive interference occurs when waves are in phase with each other. In this case the light intensity is very high (on state). In case of destructive interference there is a phase shift of 180° so they cancel each other. This tells us that the light intensity is zero (off state) [2] [5].

At some materials like LiNbO3 (Lithiumniobat), by changing the delay of the paths it is possible to control the phase shift. Because of delay mismatch between the two optical paths, there is the so-called **Drift** effect, in which the switching curve is shifted, such that the quadraturepoint of the switching curve is not at midpoint. To compensate this effect, MZMs require a bias controller. This is shown in Figure 2.3 [2] [5].

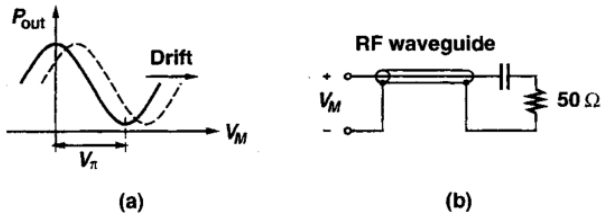

Figure 2.3: (a) Phase Drift and (b) RF Waveguide of a MZM [2]

Figure 2.4 shows the modulation and bias range of MZM. Vs is the modulation voltage, which represent the difference between on-off state voltage supplied by the modulation driver. It equals the voltage swing across the modulator. The bias voltage V_B is the average voltage (DC component) supplied by the driver [2].

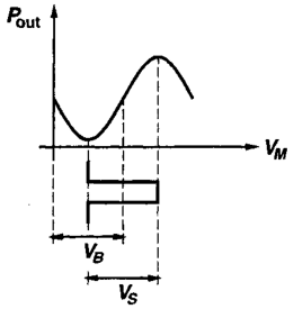

Figure 2.4: Modulation and Bias Voltage of MZM [2]

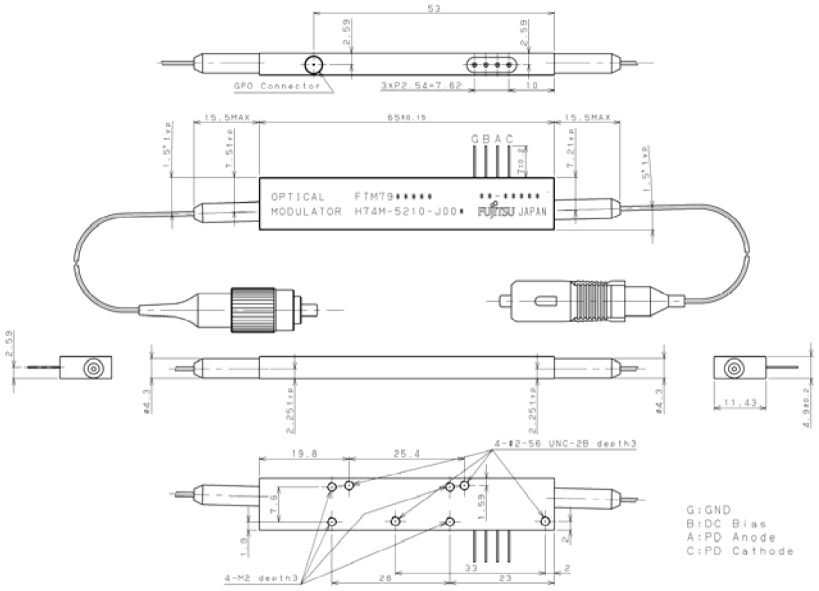

Figure 2.5: Mach-Zehnder Modulator

Figure 2.5 shows in detail the representation of the MZM. The modulator has four connections, two are for the bias voltage and two for the monitoring diode, which allows us to monitor the bias voltage. The RF-input is used for supplying the modulated electrical signal. Driving voltage from $4 - 5V$ around 10 Gbps are in the telecom window at 1550 nm. For more details please refer to Appendix A.2

2.2 Modulation Techniques

Modulation technique are very important in communication systems. Before selecting the right one, there are some criteria to be considered, like power efficiency, bandwidth efficiency, transmission reliability ect. It is a process of imprinting data on the carrier beam parameters. The optical signal parameters are characterized in amplitude, phase, frequency, and polarization of the optical carrier. FSO systems use different modulation techniques. The intensity modulation (IM) is the most used method, since it simplifies the demodulation at the receiving side with a simple use of a photodiode [5].

2.2.1 On Off Keying

On-Off Keying (OOK) is the most commonly used IM/DD technique. It is simple and widely used technique in FSO systems, in which the intensity of an optical source is directly modulated by the information sequence. It has advantages in implementation, simplicity and it is very cost effective [14]. OOK uses basically two methods: **Non-Return to Zero (NRZ)** and **Return to Zero (RZ).**

NRZ: Is the more common one because of its simplicity. The transmitter emits a rectangular pulse of duration $\frac{1}{R_b}$, where R_b is the bit rate, and an intensity $2P$ which describes the transmission power. When the signal is on, it stays on its bit period over the entire time. The bandwidth required by OOK is approximately $Rb = \frac{1}{T}$, the inverse of the pulse width [14] [15].

RZ: This method is more preferred in high-speed and long-haul transmission. The difference between the RZ and NRZ is in the transmission of one because the pulse does not remain high for the entire period. It means that only the partial duration of the bit is pulse occupied. With a $\gamma = 0.5$ the pulse width is exactly half of the period duration. This is shown in Figure 2.6. This means that OOK-RZ needs less energy than OOK-NRZ for the same performance, but it has a higher bandwidth requirement. At $\gamma = 0.5$ the double bandwidth is already used, and at $\gamma = 0.25$ already the amount of four. At the end, the choice boils down to deciding if we prefer bandwidth efficiency or energy efficiency [14] [15].

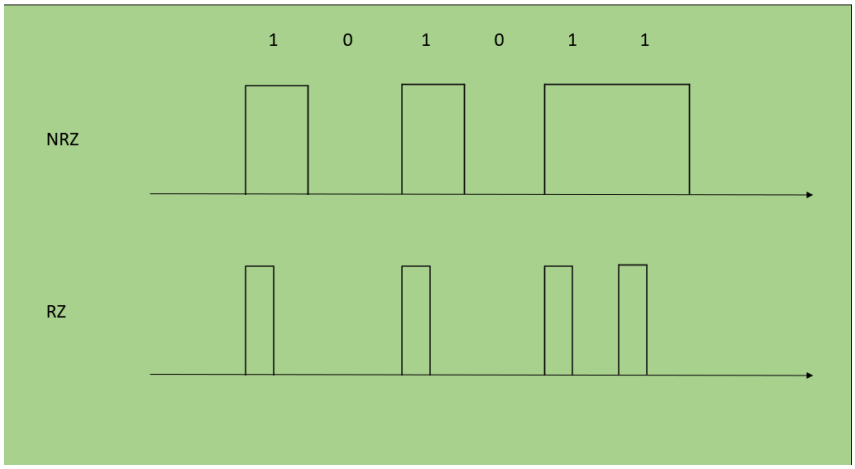

Figure 2.6: On-Off-Keying: NRZ and RZ

2.2.2 Pulse Position Modulation (PPM)

When we talk about Pulse Position Modulation (PPM), obviously we talk about Single-Pulse Position Modulation(L-PPM). PPM cover many different processes, including Multiple PPM (M-PPM) or Differential (L-DPPM). In fact, all these modulation variants offer the same advantages, especially the high power efficiency, transmission efficiency and the good security against interference that make PPM popular and a widely used modulation technique in optical communications systems. Compared to OOK, PPM has a low average power and a high peak power, this leads to good security and a high SNR features [3][14]. Furthermore We go into details to describe the principles of each variant of PPM.

Single-Pulse Position Modulation (L-PPM): is a binary n-bit data group with fix L time slots. A time slot is known as a chip. All chips are 0 except one which is 1. This gives us L different symbols. Each symbol corresponds to a bit pattern and thus results in the mapping for the transmission. L-PPM has a very good power efficiency, but it requires a higher bandwidth. The required bandwidth can be easily determined which corresponds to the number of chips. In order to maintain the advantage of power efficiency and to meet the bandwidth requirements, many variants were created [16] [3] [14]. Figure 2.7 shows an example of 4PPM of the mapping code L-PPM modulation technique:

$$\Phi : l = m_1 + 2m_2 + \cdots + 2^{n-1}m_n, n \in (1, 2, \cdots, n) \in (1, 2, \cdots, n) \tag{2.2}$$

$M = (m_1, m_2; \cdots, m_n)$ n-bit data group. If M=(0,0), then 1=0; M=(1,0), then 1=1; M=(0,1), then 1=2; M=(1,1), then 1=3 1=0,1,2,3, which present the slot position shown in Figure 2.7 [3].

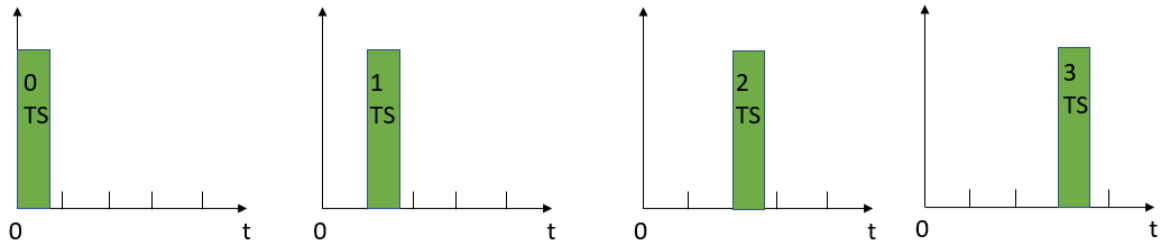

Figure 2.7: Single-Pulse Position Modulation (L-PPM) (modified from [3])

Differential Pulse Position Modulation (L-DPPM) is the improved version of L-PPM. Here the bit value is fixed, one bit is 1 and the other bits are 0. There are two types of errors that can occur. If a 0 is detected as a 1 this will be recognized as an additional symbol and the actual symbol is detected as another symbol. The second type of error is if a 1 is detected as 0, in this case the symbol is not recognized and the next one will be detected incorrectly. Of course, there can be a combination of these two error types, but the biggest problem is that these errors are only detected if a sequence of 0 is greater than (L-1) chips. Figure 2.8 shows that DPPM removes the signal behind the high signal of a PPM modulation for a code group. Compared to L-PPM, L-DPPM requires higher power consumption, but smaller bandwidth requirement [3] [14].

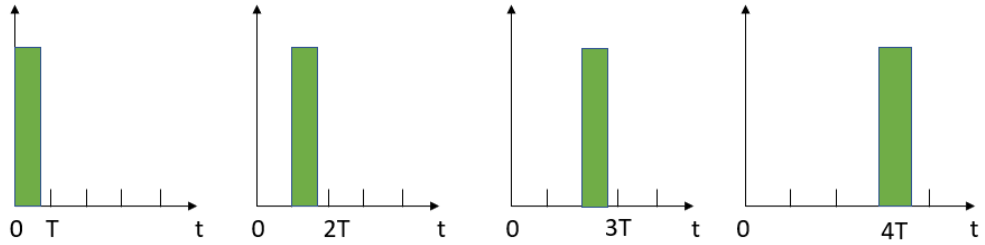

Figure 2.8: Differential Pulse Position Modulation (L-DPPM) (modified from [3])

Multi-Pulse Position Modulation (M-PPM): has fixed size of chip symbols, except that here, are more 1 pulses per symbol. Figure 2.9 shows a dual pulse PPM modulation. This modulation variant has the advantages of very good bandwidth efficiency. However, on the other side, it requires more power. When using M-PPM, not all possible symbols are used. There are two types of M-PPM: multi-pulse combination PPM and multi-pulse arrangement PPM [3] [14]. For example: two pulse position as l_1, l_2, then

$$(l_1, l_2) = \varphi(u_1, u_2, \ldots, u_n); l_1, l_2 \in \{0, 1, \ldots, M-1\}, u_f \in (0,1) \in (2) \tag{2.3}$$

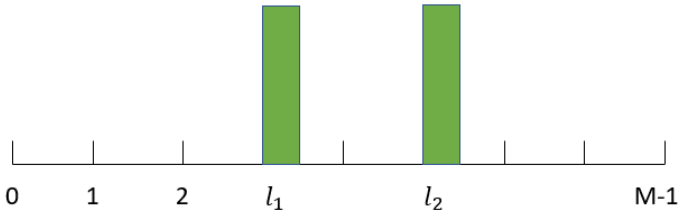

Figure 2.9: Multi-Pulse Position Modulation (M-PPM) (modified from [3])

2.3 Optical Receiver

The function of an optical receiver is to recover the transmitted data from the received optical signal. It consists of a receiver telescope, optical filter, photodetector, amplifier, and demodulator (see Figure 2.1). The system design is very similar to that from a fiber based receiver. The design of an optical receiver depends on several factors: the modulation format, hardware availability, reliability, cost efficiency and receiver sensitivity [4]. Chapter 5 introduce the design of the optical receiver and its characteristics.

2.3.1 Optical Filter

The optical filter is used to minimize the amount of background noise. Noise is a broadband signal and the use of filters can reduce this noise effect. There are used to allow the transmission of light for different wavelength. Optical filters can be developed from an Interferometer or Fiber Bragg Grating (FBG) [4] [13].

2.3.2 Optical Detectors

An optical receiver should be able to detect a low level optical signal without showing many errors. Noise is one of the important factors that give rise to bit errors, which means for a digital system it is important that the SNR is sufficiently high to yield an acceptable BER [5]. In FSO communication systems we have two types of detectors:

Communication Detectors

Beacon detectors

Application	Detector type	Material
Communication	APD	Silicon, InGaAs, InGaAsP
	PIN	Silicon, InGaAs, InGaAsP
	CCD	Silicon
	PMT	Solid-state silicon photo-cathode
Beacon(acquisition and tracking)	CCD	Silicon
	CID	Silicon
	QAPD	Silicon
	QPIN	Silicon, InGaAs

Table 2.1: Communication and Beacon detectors [4]

Some conditions to choose the right optical detector are: high sensitivity at the operating wavelength, high fidelity, large detection area, short response time, minimum noise, large electrical response to the received optical signal, low cost, small size, and high stability and reliability [5]. The main part of an optical receiver is the photodetector. It converts an optical signal into its equivalent electrical signal through the photoelectric effect [13]. The two most commonly used types of photodetectors are: **P-I-N photodetector** and **Avalanche Photodetector (APD).**

P-I-N

They are made from Si, InGaAs (preferable for longer wavelength up to $1.7 - \mu m$), and InGaAsP. P-I-N photodetector is the simplest detector, also known as p-i-n photodiode (see Figure 2.10 (a)). It consists of a p-n junction intrinsic (i) (i.e., undoped) region in between the n and p-doped material. The p-i-n photodiode is reverse biased and can operate at voltages in the range from 5 to 10V. PIN photodiode has a high resistance, as the intrinsic (i) region has no free charges. Therefore, the applied voltage is reversed at the intrinsic (i) region. Since this region is wider, the incoming photons have better probability than in the other two regions [2] [5]. The diode has two connections, the

connection on the p-zone (Anode (A)) and the connection on the n-zone (Cathode (K)). The current flow from p-zone to n-zone or from the anode to cathode. In Figure 2.10 (b) the electrodes are shown in black and anode has the form of a ring (with 2 opposite parts of it). Cathode is a flat electrode where the positive pole of the reverse bias is connected. At the top of p region is the anti-reflection coating.

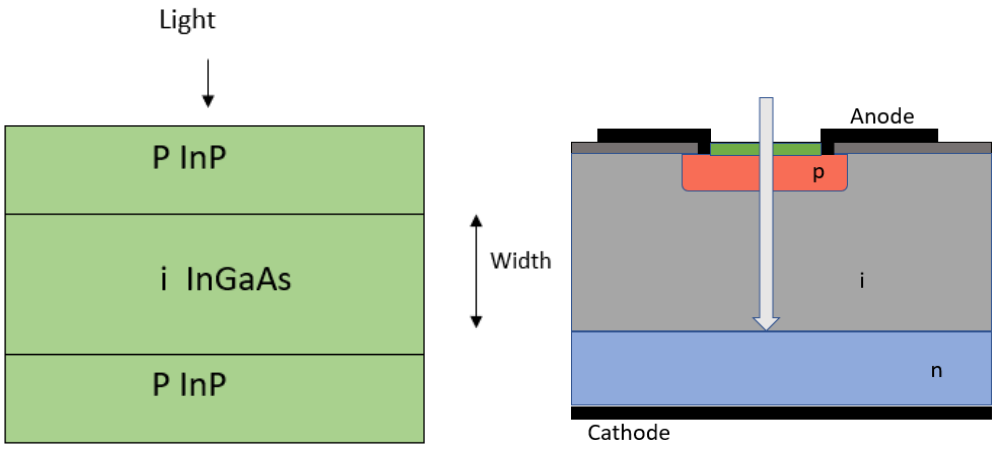

Figure 2.10: P-I-N Photodetector (modified from: [2])

APD

APD is a reversed bias diode that operates at high voltage of about 40 to 60 V. They are high sensitivity, high speed semiconductor light sensors. The structure of an APD is shown in Figure 2.11 (a). It is similar to that of an P-I-N photodetector, but it has an additional layer, the *multiplication* region.

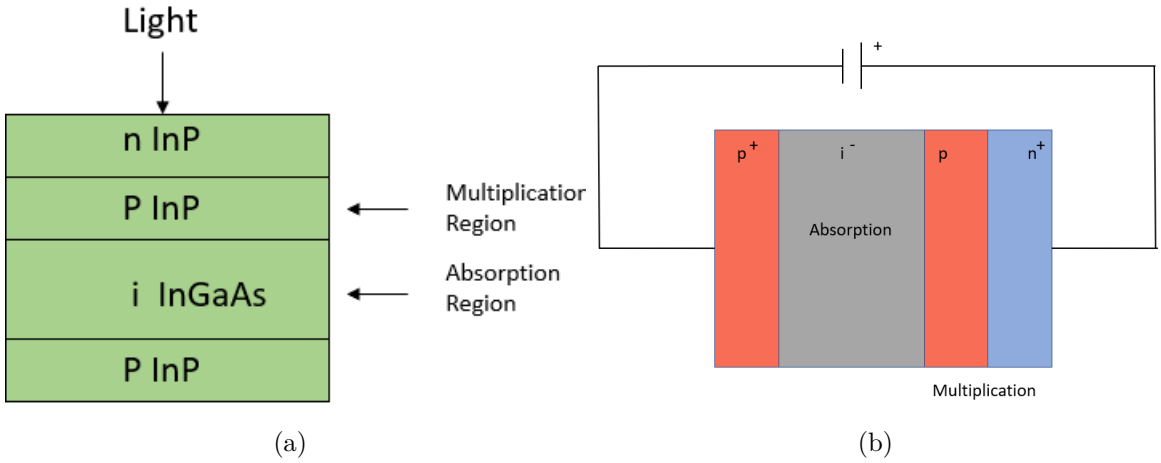

Figure 2.11: Avalanche Photodetector (modified from: [2])

The multiplication region permits the avalanche multiplication of the electron-hole

pairs generated in the i-layer, known as the absorption region see Figure 2.11 b). Depending on their operating wavelength, APD provides low noise, good quantum efficiency, low dark current, high sensitivity etc. Besides these qualities we have to mention that the noise performance is very poor which results that Si devices outperform the longer wavelength devices even with low quantum efficiency [4] [2]. Chapter 5 introduce the used optical receiver which uses an APD sensor capable of receiving data rate up to 10Gbps.

3. Laser Standards and Classifications

Before designing a FSO link, it is important to consider all the necessary parameters. IR (Infrared), UV (Ultraviolet) and visible light radiation can affect the eye and make irreparable damages if the safety standards are not taken into account. There are rules and security levels in order to prevent these risks that can affect our skin and eyes. Because of these safety risks, it is crucially important to choose the appropriate wavelength [5].

3.1 Eye Safety and Regulations

Near and far infrared radiation can cause cornea damage. The eye is very sensitive to UV radiation. Even short exposure can be painful for the eye. Near UV wavelength are absorbed in the lens which affect the eye and the vision is blurred. Photokeratitis is a painful condition caused by damage to the eye from far UV and IR regions, it is like having a sunburned eye. Since the light is absorbed in the cornea, i.e., the clear front window of the eye that lead to pain, different wavelengths radiation can cause different effects. Visible and Near IR region can damage the retina of the eye, thus leading to permanent loss of the vision. The medium wave UV causes skin burns, erythema (reddening of the skin) and darkening of the skin [4]. Figure 3.1 shows the different region of explosion for the human eye. For wavelengths higher than > 1400 nm the absorption coefficient of the cornea is much higher than for wavelengths < 1400 nm. The cornea is opaque to infrared radiation over $1.4\mu m$, therefore in the $1.55\mu m$ region we can avoid the restricted standards for eye safety regulations [4]. Figure 3.2 shows the absorption of light as function of wavelength.

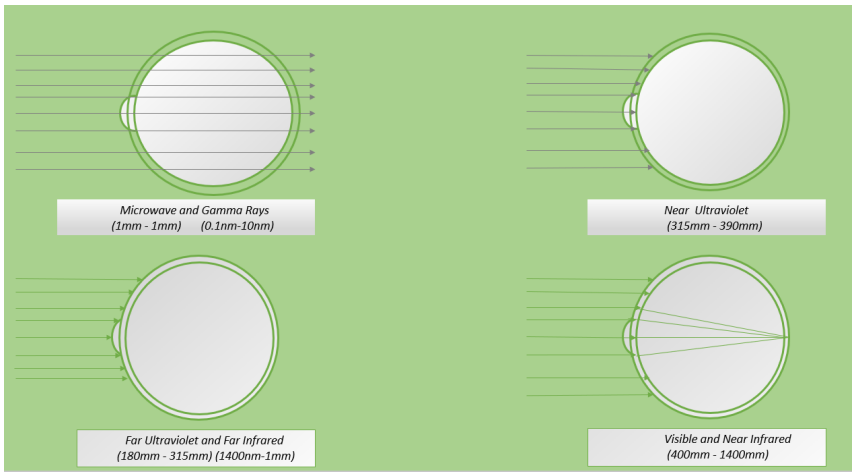

Figure 3.1: Different region of explosion for the eye (modified from [4])

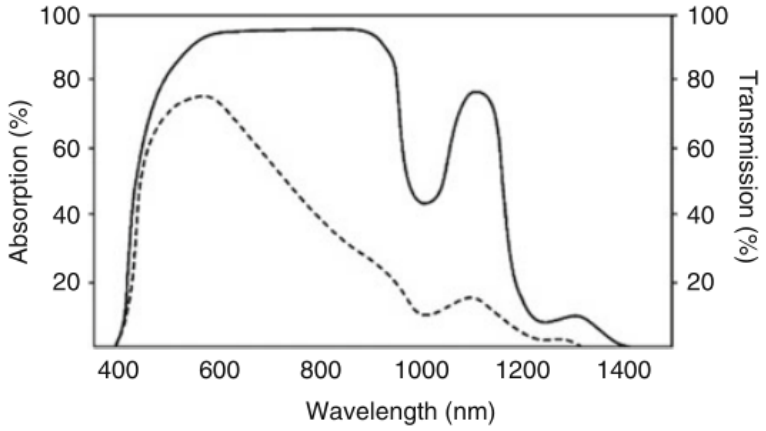

Figure 3.2: Absorption of light as function of wavelength [4]

3.2 Optical Sources

Optical sources are characterized with their power consumption and radiation pattern. The most used ones are LEDs and LDs. For long distance communication , LDs are preferred for the fact that the energy from a laser source is collimated [5]. We have two types of sources for the optical communication system (see Figure 3.3)

Extended Source: The emitted light from the device radiates in all directions or within a very wide angle.

Point Source: The radiated energy from the device emits within a very low angle [5].

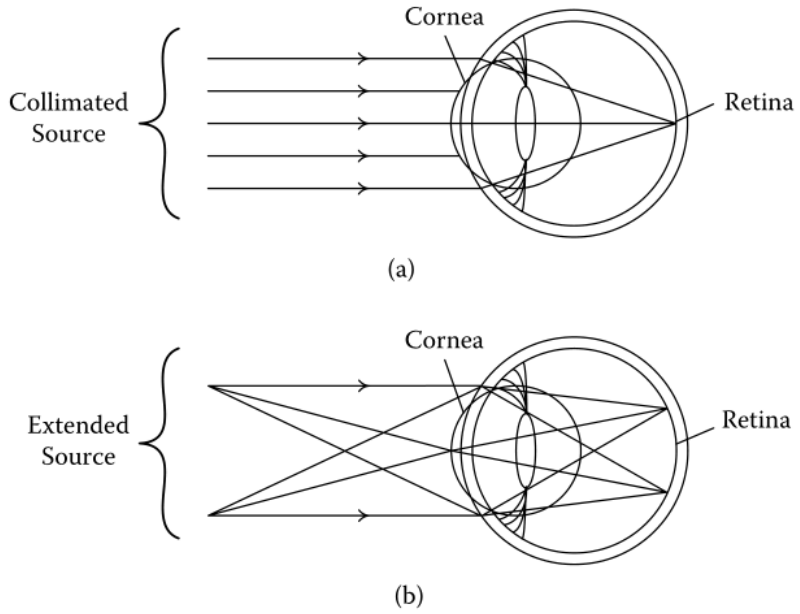

Figure 3.3: Eye transmission for: (a) point source and (b) extended source [5]

.

3.3 Laser classification according to IEC and ANSI standards

The laser classification system is based on the output power, wavelength and pulse duration. There are standards in different countries which are regulated by the European Committee for Electrotechnical Standardization (ECES). For more information, please refer to [4, p.35] where you can see in details the principle of laser safety standards for: International Electrotechnical Commission (CENELEC) and American National Standards Institute (ANSI) Z136.

3.4 Accessible Emission Limits according to IEC standard

IEC describes the accessible exposure limits (AELs) and shows that the required warning labels for different types of radiation are safe.

Laser classification	Average Output power optical power (mW)	
	850nm	1550nm
1	<0.22	<10
2	Used only for 400-700nm and has the same AEL as class 1	
3R	$0.22 - 2.2$	$10 - 50$
3B	$2.2 - 500$	$50 - 5004$
4	>500	>500

Table 3.1: Accessible Emission Limits for 850 nm and 1550 nm [4]

Classification	Power (mW)	Aperture size (mm)	Distance (m)	Power density (mW/cm^2)
Class 1	10	7	14	26
		25	2000	2.04
Class 1M	10	3.5	100	103.99
	500	7	14	1299.88
		25	2000	101.91

Table 3.2: Requirements of Class 1 and 1M laser classification [4]

4. Link Analysis

4.1 Link Budget

Link analysis relates the transmitted power and the received power and shows in detail how the difference between these two is accounted for. The purpose is to determine if a communication link can support the target data rate, and if so with what margin. Using matlab software we simulated and analyzed the system by calculating the basic formulas, which are related to the link budget [17]. First we introduced the link budget and calculated the free space losses and the optical received power. Link budget simulation of the received power signal and SNR is shown in Figure 4.4 and 4.3, and shows if a communication could be successful or not. The case here is not for terrestrial communication, but for ground to satellite communication.

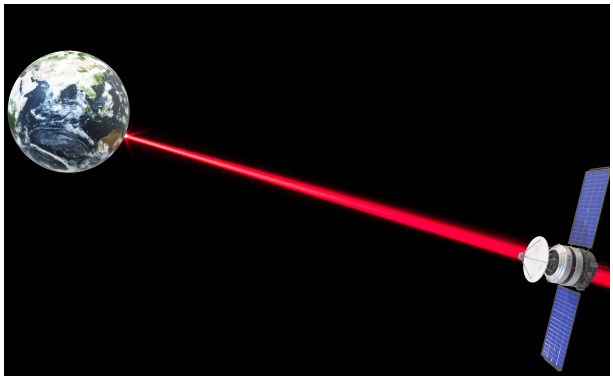

Figure 4.1: Laser Space Communications System

A link budget has at least three entries, one for the transmitter, one for the channel, and one for the receiver [18]. This is shown in Table 4.1

Item	Value	dB value
Average Transmitter Power	1.0 mW	0.0dBm
Propagation Losses	1%Transmission	−20dB
Signal Power at Receiver		$-20dB$
Receiver Sensitivity		−30dB
Power margin		+10dB

Table 4.1: Link Budget entries

The flux density $S(W/m^2)$ of an isotropically radiating antenna at a given distance d, can be calculated using the following formula [18, p. 61]:

$$S = \frac{P_t}{4 \cdot \pi \cdot d^2} \tag{4.1}$$

where P_t is the Optical Transmitted Power, A_e is the Effective Area, λ is carrier wavelength and G_r is the receiver gain.
Directivity D, describe how much of the light's energy is concentrated in a specific direction, where gain G is given by the multiplication of the radiation efficiency and the directivity

$$D = \frac{4 \cdot \pi \cdot Ae}{\lambda^2} \tag{4.2}$$

$$G = \eta \underset{rad}{\cdot} D \tag{4.3}$$

$$G_r = \frac{4 \cdot \pi \cdot Ae}{\lambda^2} \tag{4.4}$$

Isotropic Equivalent Radiated Power (EIRP) is an important parameter for the link budget tool. This is defined as the power that an isotropic source would have to emit, to have the same power flux. It is described by:

$$EIRP = P_t \cdot G \tag{4.5}$$

4.2 Transmission Losses

<table>
<tr><td rowspan="5">Transmission loss</td><td rowspan="5">Propagation Losses</td><td colspan="3">Free Space Losses</td></tr>
<tr><td rowspan="4">Atmospheric Losses</td><td>Ionospheric effects</td><td>Scintillation effects</td></tr>
<tr><td rowspan="3">Tropospheric effects</td><td>Attenuation</td></tr>
<tr><td>Rain Attenuation</td></tr>
<tr><td>Gas absorption</td></tr>
<tr><td></td><td></td><td></td><td>Sky Noise</td></tr>
</table>

Table 4.2: Transmission losses

Losses are a major problem when it comes to transmission in satellite communication. We have different kind of losses from different sources like: free space losses, atmospheric losses (troposphere and ionosphere losses), pointing losses, equipment and environment losses ect. This work here is focused on Free Space Losses and additional losses will be estimated.

4.3 Free Space Losses (FSL)

Free space means air, vacuum, outer space, where light is propagated in this medium to transmit the information. Free Space Path Loss (FSPL) is the loss in strength of an electromagnetic signal as it travels through free space in a line-of-sight path [6]. In order to calculate the FSL we have to find the maximum distance between the Satellite (ST) and the Ground Station (GS) [6]. This is shown in Figure 4.2.

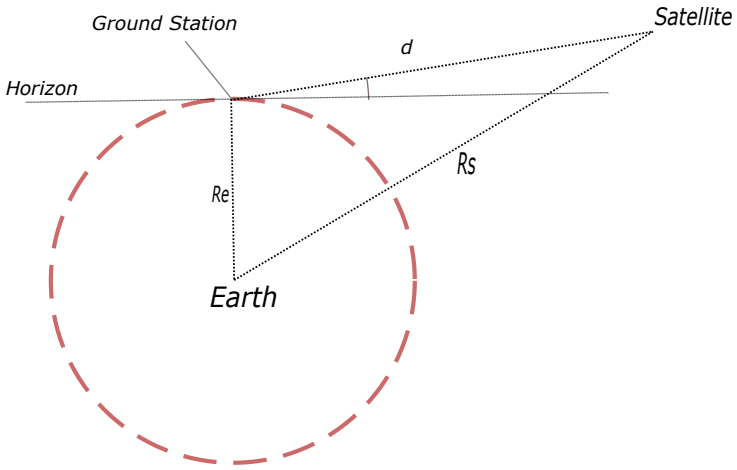

Figure 4.2: Variation distance between Satellite and Ground Station (modified from [6])

$$Rs^2 = d^2 + Re^2 - 2 \cdot d \cdot \cos(\Theta + \pi \cdot 2) \tag{4.6}$$

$$d = -Re\sin(\Theta) + \sqrt{Re^2\sin(\Theta) + Rs^2 - Re^2} \tag{4.7}$$

Now we can calculate the FSL

$$FSL = L_s = \left(\frac{4\pi d}{\lambda^2}\right)^2 \tag{4.8}$$

In terms of dBs we have

$$FSL = L_s = 10\log\left(\frac{4\pi d}{\lambda^2}\right)^2 \tag{4.9}$$

where Re is the Radius of Earth, d is the distance GS-ST, Rs is the distance Earth-ST and Θ is the elevation angle.

4.4 Optical Received Signal Power

After performing all the necessary steps the optical received signal power is defined as

$$P_r = P_t \cdot G_r \cdot G_t \cdot L_s \cdot L_a \cdot \eta_{pt} \cdot \eta_t \cdot \eta r \tag{4.10}$$

$$P_r = P_t \cdot G_r \cdot G_t \cdot L_s \cdot L_A \tag{4.11}$$

$$L_A = L_a \cdot \eta_{pt} \cdot \eta_t \cdot \eta r \tag{4.12}$$

Entries in link budget are usually expressed in decibels

$$P_r = P_t + G_r + G_t - L_s - L_A \tag{4.13}$$

$$P_r = P_t + G_r + G_t - 10\log\left(\frac{4\pi d}{\lambda^2}\right)^2 - L_A \tag{4.14}$$

where P_t is the transmitter optical power, $G_{t,r}$ is the transmitter and receiver gain, L_s are the space losses, L_a are the atmospheric losses, η_{pt} pointing loss, L_A Additional losses, η_t, transmitter efficiency and η_r receiver efficiency.

4.5 Noise Power

There are three types of sources that decrease the channel capacity in the receiver. Photo electrons generated by incident background light

$$P_n^{sky} = I_b(\lambda)\delta_\lambda \Omega_{det} \frac{\pi D_r^2}{4} \eta_{det} \eta_r \eta_{pol} \tag{4.15}$$

$I_b(\lambda)$ is the incident sky radiance at wavelength, δ_λ is the narrow band filter bandwidth, Ω_{det} is the detector field-of-view , η_r is the receiver efficiency and η_{pol}polarization rejection. Dark noise electrons generated from detector

$$P_n^{dark} = 4\delta^2 l_d E_\lambda \tag{4.16}$$

where l_d is the detector dark rate, 2δ is the detector spatial width, and E_λ is the energy of a single photon of a λ wavelength.

4.6 Thermal Noise

Thermal noise is a big factor in the degradation of the signal quality. The noise is usually caused by the electronics inside the system. Noise calculation are related to power consideration. Noise Power is determined as

$$P_n = k \cdot T \cdot W = N_0 W \tag{4.17}$$

P_n is the available noise power, k is the Bolzman constant $k = 1.38062 \cdot 10^{23} \frac{J}{K}$, W is Badnwidth, $N_0 = k \cdot T$ is the noise spectral density. Noise Figure:

$$F = \frac{\frac{S}{N}in}{\frac{S}{N}out} \tag{4.18}$$

Considering all the noises that comes from resistor at the input, the temperature T_e is given by

$$T_e = T_0(F-1) \tag{4.19}$$

$$F = 1 + \frac{T_e}{T_0} \tag{4.20}$$

$$T_L = T_0(L-1)T_{RX} = T_0(L-1) + LT_{LNA} + \frac{L}{G_{LNA}} T_2 \tag{4.21}$$

where T_{T_0} is the reference noise temperature, T_{RX} is the total receiver noise temperature, T_a is the antenna temperature and T_L is the resistive loss temperature.

The System Noise Temperature is

$$T_{sys} = T_a + T_{RX} \tag{4.22}$$

4.7 Signal To Noise Ration SNR

Signal to Noise Ratio is very important for a good communication. The SNR is defined as

$$SNR = \frac{P_r}{P_n} \tag{4.23}$$

$$\frac{E_B}{N_0} = SNR \cdot \frac{B_N}{r} \tag{4.24}$$

$$\frac{C}{N} = \frac{P_t \cdot G_t \cdot G_r \cdot \lambda^2}{(4\pi r)^2 \cdot L_a \cdot k_B \cdot T_s \cdot B} \tag{4.25}$$

N_0 is the Noise power spectral density, E_B is the Bit Error Rate (BER), B_N is the Noise Bandwidth and r is the Information rate.
An increase of data rate increases the bit error rate. An increase in SNR decreases the bit error rate. Modulation scheme, also play a key issues when talking about how successful an incoming signal can be interpreted [19] [20]. Using the relation between energy per bit to noise power spectral density $\frac{E_b}{N_0}$ and the relation of SNR we get the following expression

$$\frac{E_b}{N_0} = SNR \cdot \frac{B_N}{r} = EIRP + \frac{G}{T_{sys}} - 10 \cdot \log \frac{K_B}{dB} \frac{J}{K} - 10 \log \frac{B_N}{1Hz} - 10 \log \left(\frac{4\pi d}{\lambda^2} \right)^2 - L_A \tag{4.26}$$

In fact, with this expression we can evaluate the BER. Evaluating the BER means we have information about the quality of the communication. This tells us which average amount of data will be lost. Link Margin M can be defined as

$$M = \frac{E_b}{N_0} - \left. \frac{E_b}{N_0} \right|_{req} \tag{4.27}$$

The **Link Budget** tool gives us an optimistic view about the Satellite Link and tells if the communication link will be good enough.
Table 4.3 contains the parameters used for the link budget analysis.

Formula	Parameters
Flux Density	$S = \frac{P_t}{4 \cdot \pi \cdot d^2}$
Isotropic Equivalent Radiated Power	$EIRP = Pt \cdot G$
Receiver Gain	$G = \eta_{rad} \cdot D$
Directivity	$D = \frac{4 \cdot \pi \cdot Ae}{\lambda^2}$
Effective area	$A_r = \frac{\lambda^2}{4\pi} G_r$
Transmiter Power	$P_r = S \cdot A_r$
Received Signal Power	$P_r = P_t \cdot G_r \cdot G_t \cdot L_s \cdot L_a \cdot \eta_{pt} \cdot \eta_t \cdot \eta r$
Free Space Loss	$FSL = 10 \log \left(\frac{4\pi d}{\lambda^2}\right)^2$
Dark Noise	$P_n^{dark} = 4\delta^2 l_d E_\lambda$
System Temperature	$T_{sys} = T_a + T_{rx}$
Noise power spectral density	$P_n = k \cdot T \cdot W = N_0 W$
Carrier to Noise Ratio	$\frac{C}{N} = \frac{P_t \cdot G_t \cdot G_r \cdot \lambda^2}{(4\pi r)^2 \cdot L_a \cdot k_B \cdot T_s \cdot B}$
Signal to noise ratio, or signal to noise per bit	$\frac{E_b}{N_0} = EIRP + \frac{G}{T_{sys}} - 10 \cdot \log \frac{K_B}{dB} \frac{J}{K} - 10 \log \frac{B_N}{1Hz} - 10 \log \left(\frac{4\pi d}{\lambda^2}\right)^2 - L_A$

Table 4.3: Link Budget

Using all the expressions in Table 4.3 it is possible to show a simulation of the received power and SNR as function of distance. In the given Table 4.4 the received lens diameter is very small 10 cm and the received power is around -60 dBm. The result of this simulation is shown in Figure 4.3.

Parameters	Value
Wavelength	$\lambda = 1550$ nm
Elevation	90°
Transmitter Lens diameter	20 mm
Receiver Lens diameter	100 mm
Channel length	35786 km
Data rate	100 Mbps
Transmitted power	1 W

Table 4.4: Link parameters with an received lens diameter of 10 cm

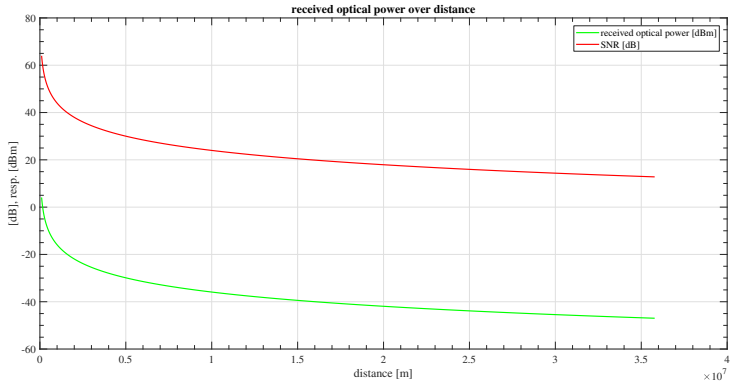

Figure 4.3: Simulation of Received Power and SNR over distance for a received lens diameter of 10 cm

In Table 4.5 the given received lens diameter is 0.5 cm and the result of this simulation is shown in Figure 4.4

Parameters	Value
Wavelength	$\lambda = 1550$ nm
Elevation	90°
Transmitter Lens diameter	20 mm
Receiver Lens diameter	5000 mm
Channel length	35786 km
Data rate	100 Mbps
Transmitted power	1 W

Table 4.5: Link parameters with an received lens diameter of 0.5 cm

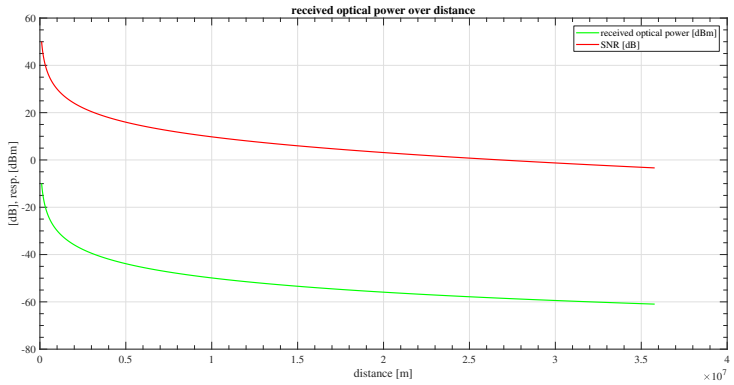

Figure 4.4: Simulation of Received Power and SNR over distance for received lens diameter of 0.5 cm

As a conclusion of the link analysis, the link budget simulation of the received power signal and SNR using the interface in MATLAB software was successfully simulated and showed that the calculation about the essential parameters and analytic formulas including the free space losses could support the target data. In the first simulation the received power was around -60 dBm and the results were not satisfied. In the second simulation the lens diameter was 0.5 cm and the received power and SNR were satisfied. Link budget is an important tool to investigate the areas, gain and losses that possibly will occur between transmitter and receiver of satellite communication system [21] [17].

5. Hardware Implementation and Analysis

This chapter introduces the practical part of this thesis, which includes the development of the optical transmitter and receiver, hardware implementation, performance analysis and results.

5.1 Optical Transmitter

The main function of an optical transmitter is to convert an electrical signal into an optical signal. Figure 5.1 shows the optical transmitter schematic created via the software program EAGLE.

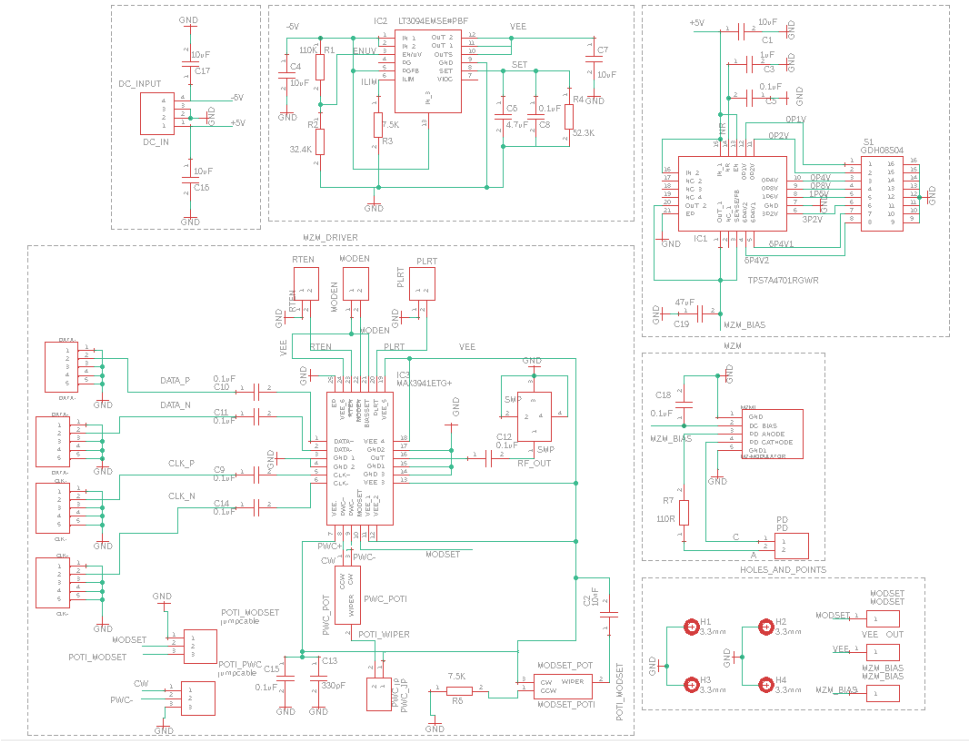

Figure 5.1: Optical Transmitter Schematic

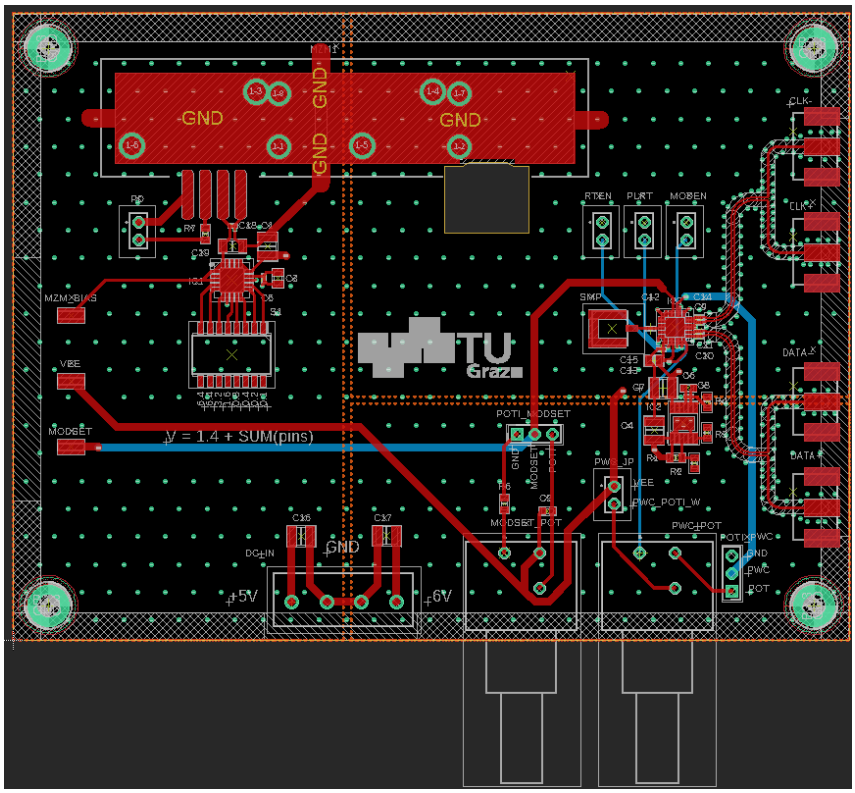

Figure 5.2: Optical Transmitter PCB Layout

The PCB is designed in a four layer board with a dimension of 120×90 mm. The stack up of the board is shown in Figure 5.3. The top and bottom layers are used for routing, and the second and third layers are used as ground and power planes, respectively.

Figure 5.3: Four Layers Stack-up Board of TX and RX. The green parts represent the copper layers, while the gray parts represent the dielectric material.

The MZM driver operates with a data rate up to 10.7 Gbps and has a rise edge speed of 23 ps with an integrated bias network. A negative LDO is used because the driver required a negative supply. The reason to choose the negative linear regulator LT3094 (see [22]) is, because of its low noise characteristic. The positive linear regulator has an input voltage range from +3 V to +36 V , and for similar reasons as the negative LDO, the choice of TPS7A4700 is due to its low noise characteristic. The capacitors 0.1 uF and 10 uF are used as filters to reduce noise, which can be seen almost on every part of the board.

It is important to place this capacitors as near as possible to the driver. The capacitors C9, C10, C11, C14 are used as DC blocking capacitors. The MZM has an SMP interface, which require the use of an SMP cable. Therefore, an SMP connector is used at the output of the driver. Thereafter, the driver and MZM are connected with an SMP assembly cable, which has a bandwidth up to 26.5GHz.. The potentiometers shown in Figure 5.10 are used to control the PWC (Pulse Width Adjustment) and MODSET (Modulation Current Set)of the driver. The several jumpers on the design are used to control several pins.The rectangular hole seen in the schematic which is next to the modulator is there to ensure that the cable can move freely. The test points VEE, MZM BIAS and MODSET seen on the left side of the board are used to monitor the DC voltages. For more details please refer to [23].

5.1.1 Matching Parameters

Figures 5.4 and 5.5 show the matched transmission lines used in both transmitter and receiver boards. Matching is one of the most important steps to have an appropriate RF interconnect. The structure used here is a grounded coplanar waveguide. In coplanar waveguides the signal trace and the ground are located at the same layer. By including a ground plane underneath the signal trace, the structure is referred as grounded coplanar waveguide. The design parameters of a coplanar waveguide can be obtained e.g., by using an online calculator by providing it with the necessary parameters. Figure 5.4 shows the stack up of a grounded coplanar waveguide, while Figure 5.5 shows the stack up of a differential grounded coplanar waveguide. Furthermore, Table 5.1 and Table 5.2 show a list of the design parameters of both structures.

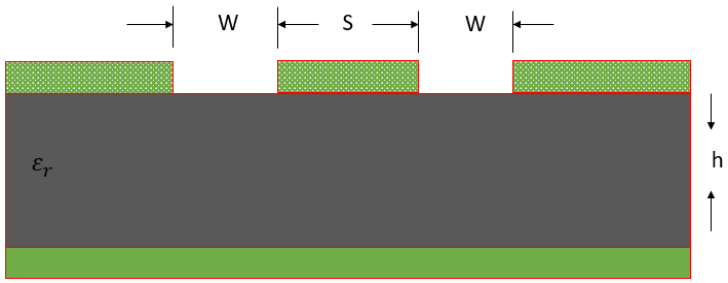

Figure 5.4: Stack up layer of a grounded coplanar waveguide

Input Data	Results
Relative Dielectric Constant	3.66
Trace Width (S)	0.3176 mm
Clearence (W)	0.2 mm
Dielectric Thickness	0.1702 mm
Characteristic Impedance	50Ω

Table 5.1: Matching Parameters for a Characteristic Impedance of 50Ω

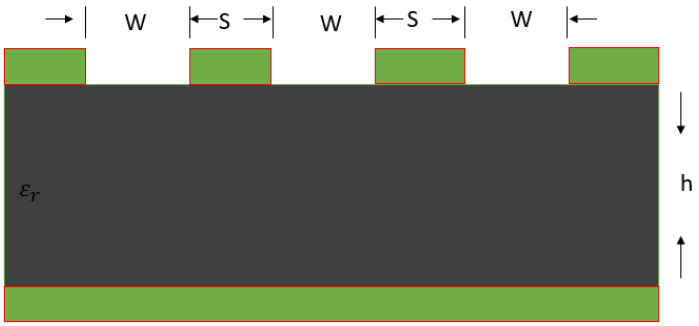

Figure 5.5: Stack up layer of a differential grounded coplanar waveguide

Input Data	Results
Relative Dielectric Constant	3.66
Trace Width (S)	0.2516 mm
Clearence (W)	0.2 mm
Dielectric Thickness	0.1702 mm
Characteristic Impedance (differential)	100Ω

Table 5.2: Matching Parameters for a Characteristic Impedance of 100Ω

5.1.2 MZM Driver

Figure 5.6 shows the schematic and layout of MZM driver. It has many suitable characteristics like: On-Chip Bias Network, 23ps Edge Speed, Programmable Modulation Voltage Up to 3Vpp, Programmable EAM Biasing Voltage Up to 1.25V, Integrated Modulation and Biasing Functions, Pulse-Width Adjustment, Enable and Polarity Controls [23].

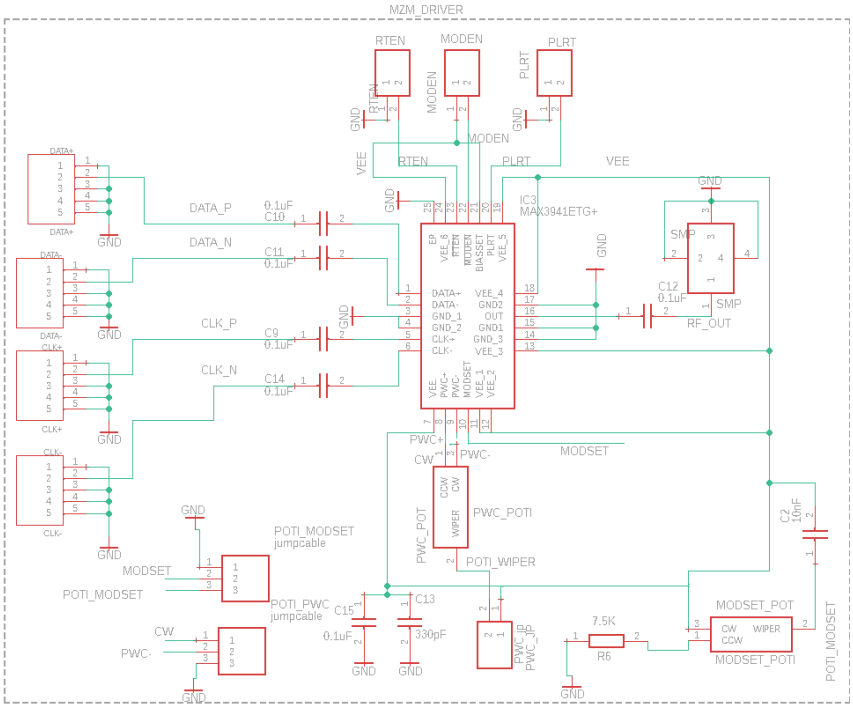

(a)

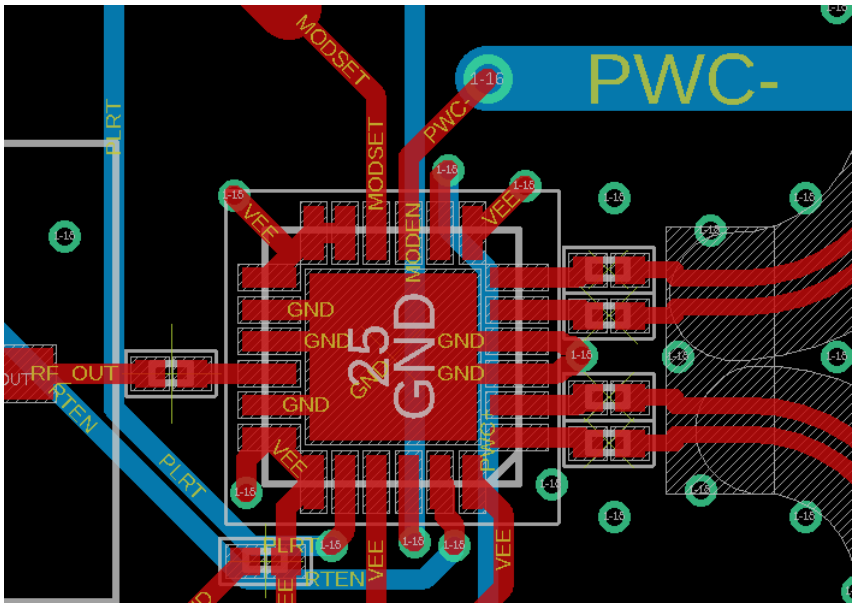

(b)

Figure 5.6: Optical Driver

The Power-Supply Voltage is denoted as VEE and has the values from $-5.5Vto-4.9V$.

For more details please refer to [23].

$$V_{MOD} = I_{MOD} \cdot \frac{Z_L \cdot R_{out}}{Z_L + R_{out}} \tag{5.1}$$

$$V_{BIAS} = I_{BIAS} \cdot \frac{Z_L \cdot R_{out}}{Z_L + R_{out}} \tag{5.2}$$

5.1.3 MZM

Figure 5.7 and 5.8 shows the board and schematic layout of MZM. The MZM is a single ended modulator with a data rate up to 10 Gbps. The pin out of the modulator consist of DC bias (pin 1 and 2) and a monitoring photodiode (pin 3 and 4). The RF signal is supplied over an SMP coaxial connector. For more details on MZM see chapter 2 in section 2.1.3.

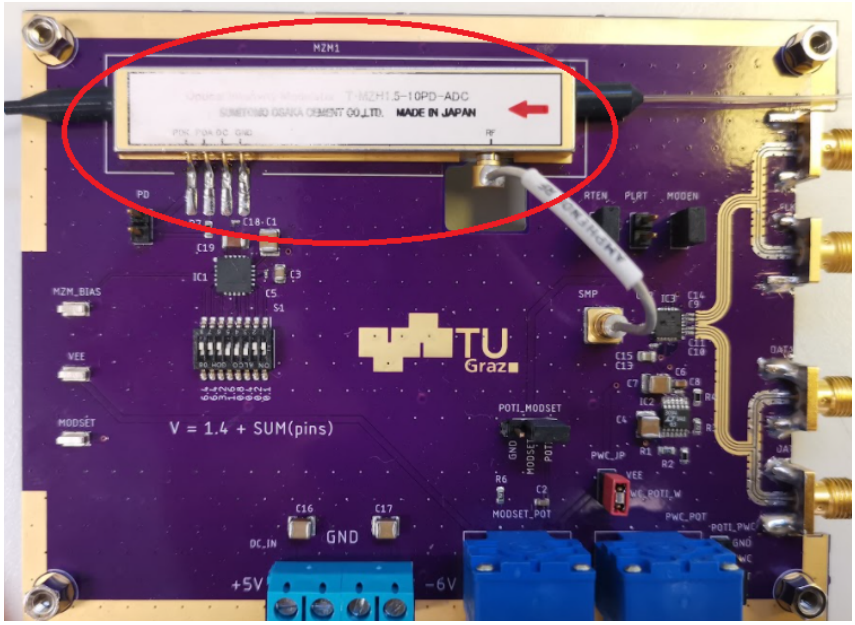

Figure 5.7: MZM on Transmitter Board

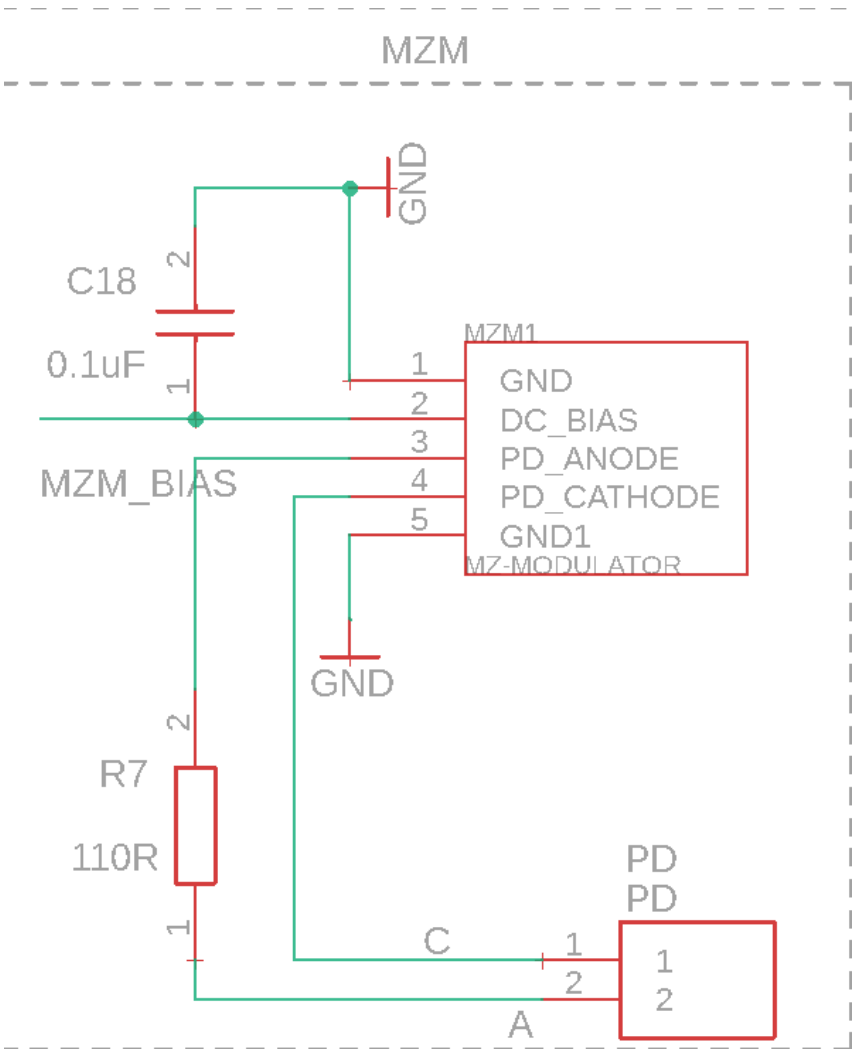

(a)

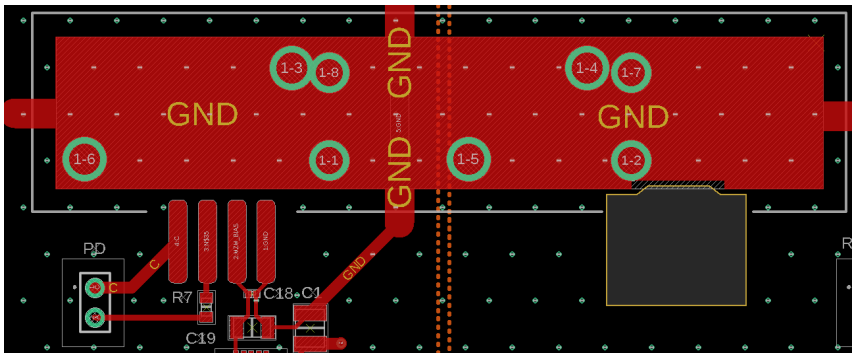

(b)

Figure 5.8: MZM Schematic and PCB Layout

Figure 5.9 shows the four layers of the optical transmitter, where top and bottom layers are used for routing, and the second and third layers are used as ground and power planes, respectively.

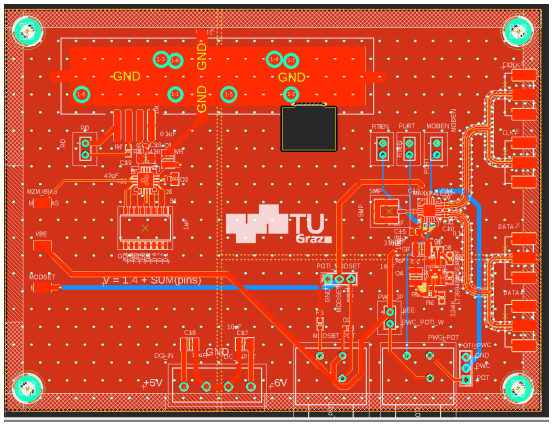

(a)

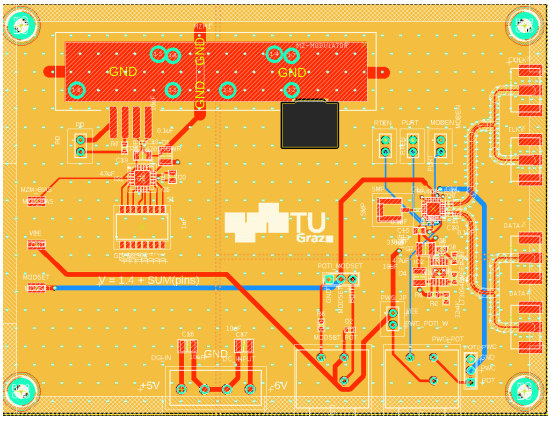

(b)

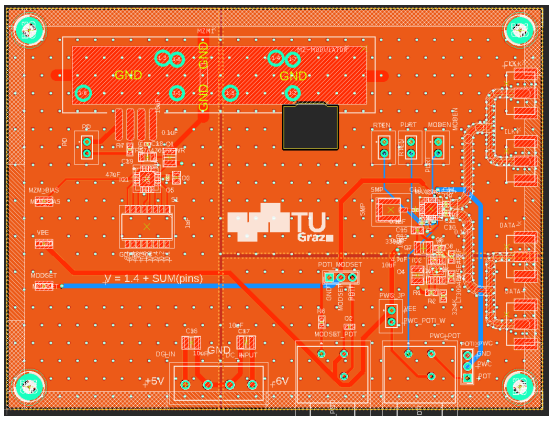

(c)

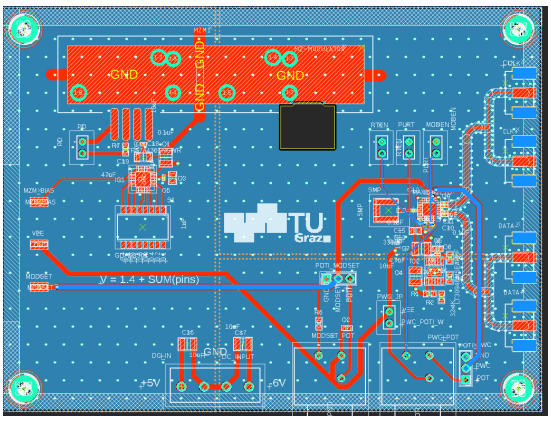

(d)

Figure 5.9: Optical transmitter four layer board: a) Top b) Ground c) Power and d) Bottom

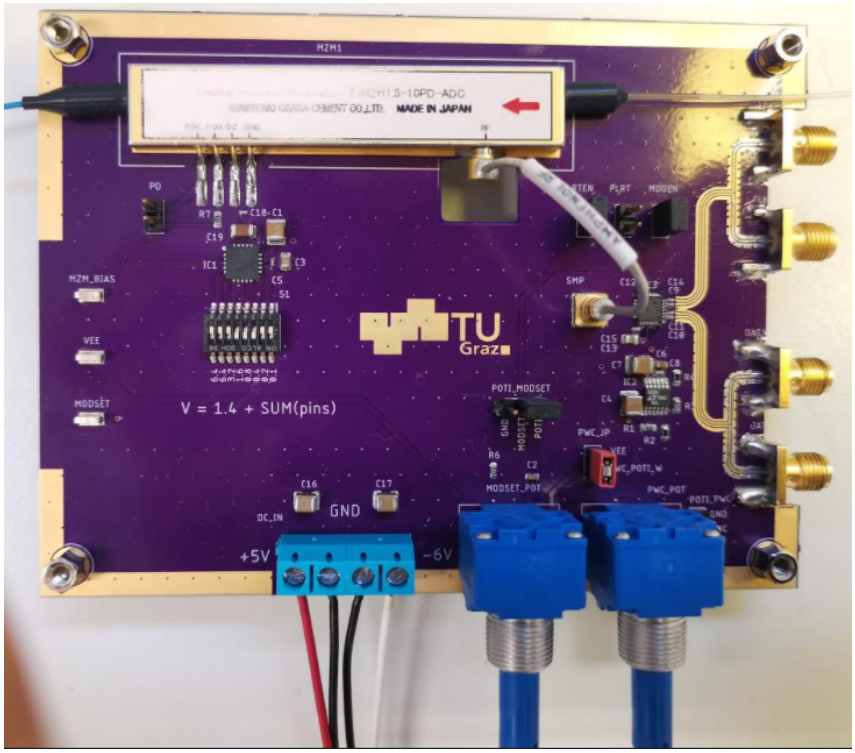

(a)

(b)

Figure 5.10: Final hardware of the optical transmitter

5.2 Optical Receiver

The main function of an optical receiver is to recover the transmitted data from the received optical signal. Figure 5.12 shows the PCB design of the optical receiver.

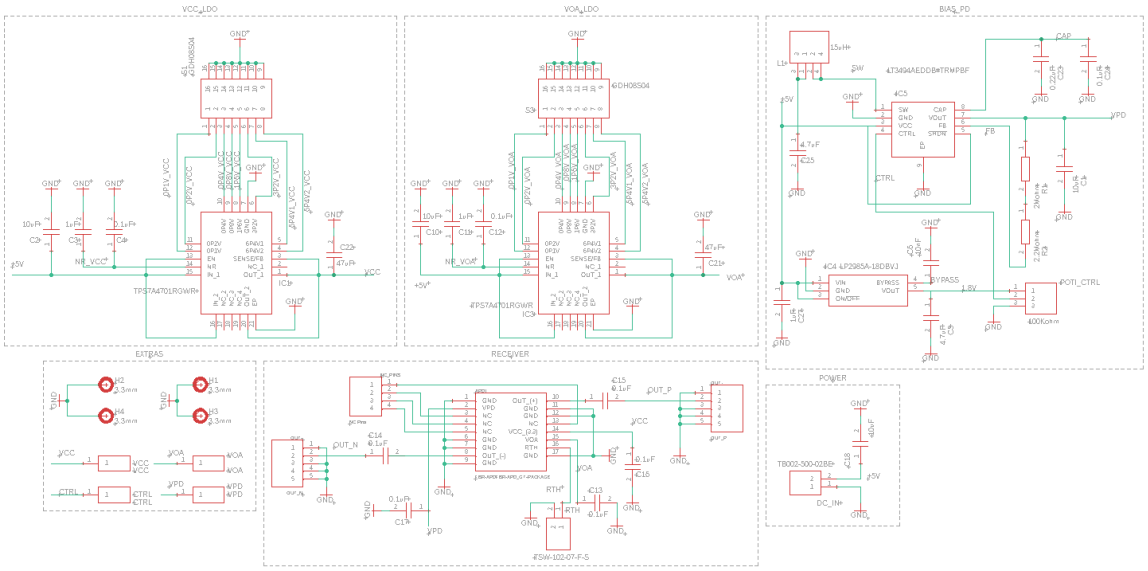

Figure 5.11: Optical Receiver Schematic

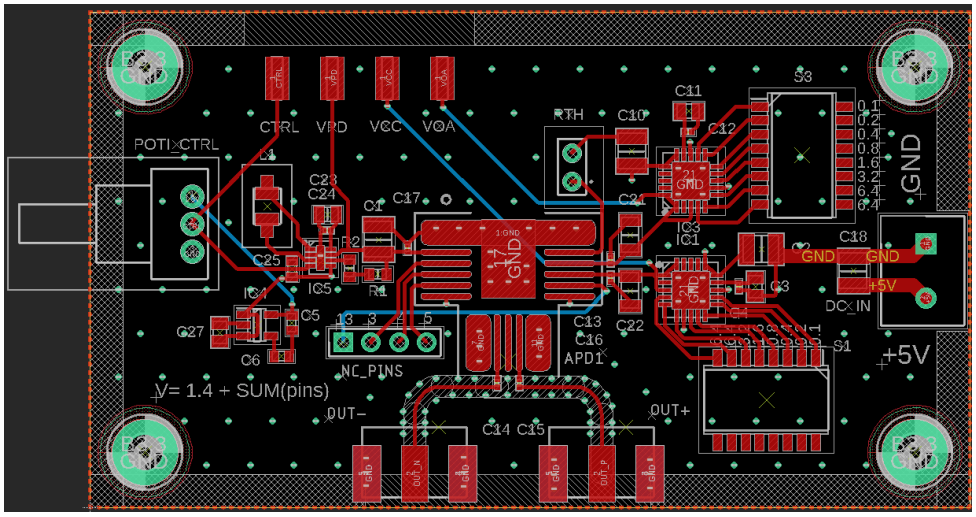

Figure 5.12: Optical Receiver Layout

For the receiving sensor, an APD is used, which is capable of receiving data rate up to 10 Gbps. The device model is FiBest-FBR2178GB, which requires a bias voltage of around 29 Volt. It also has an integrated Trans-Impedance Amplifier (TIA) that requires a supply voltage of 3.3 V. The board layout is shown in Figure 5.12: the left side shows the DC-DC converter, which is to provide 29 V for the biasing of the APD, and the right side shows the LDO for the TIA. On the board, it is also included another LDO for VOA

(variable optical attenuator) but unfortunately the device model does not support this feature. Matching of the input ports has the same parameters as used in Table 5.1. The potentiometer seen on the left side is used to control the bias voltage.

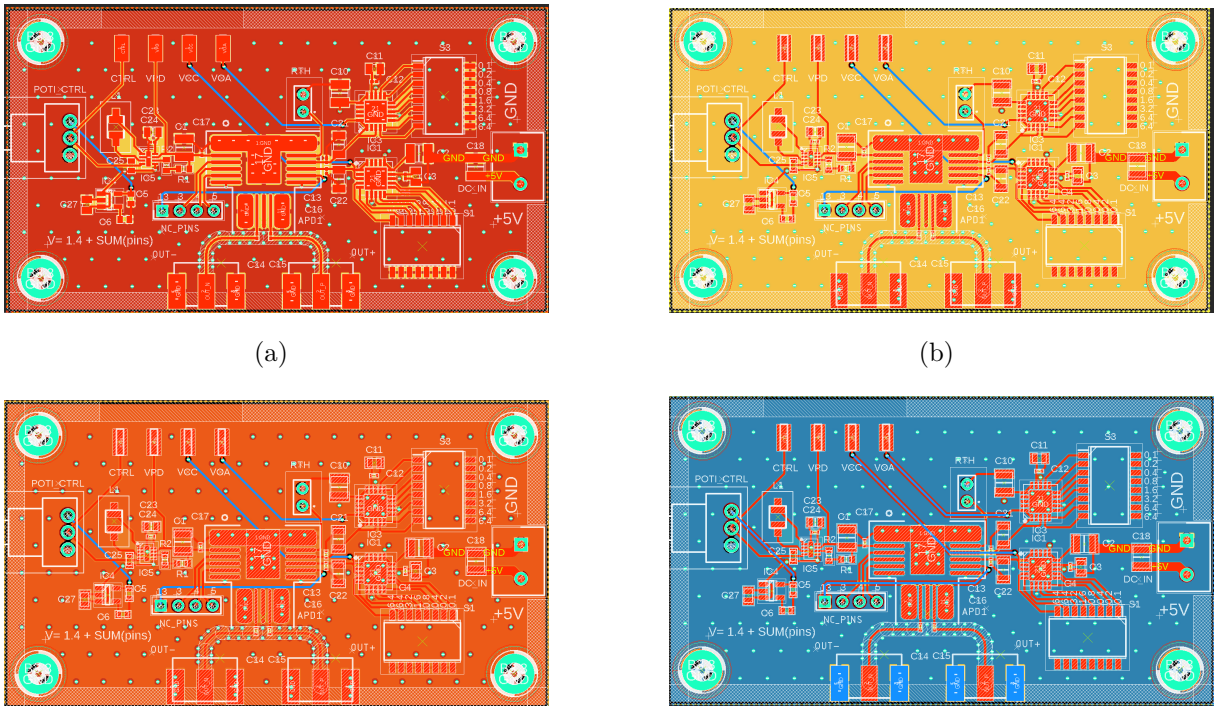

(a) (b)

(c) (d)

Figure 5.13: Optical Receiver four layer board: a) Top b) Ground c) Power d) Bottom

The stack up of the board is shown in Figure 5.5. The individual layers are shown in the Figure 5.13. The top and bottom layers are used for routing, and the second and the third layers are used as ground and power planes, respectively.

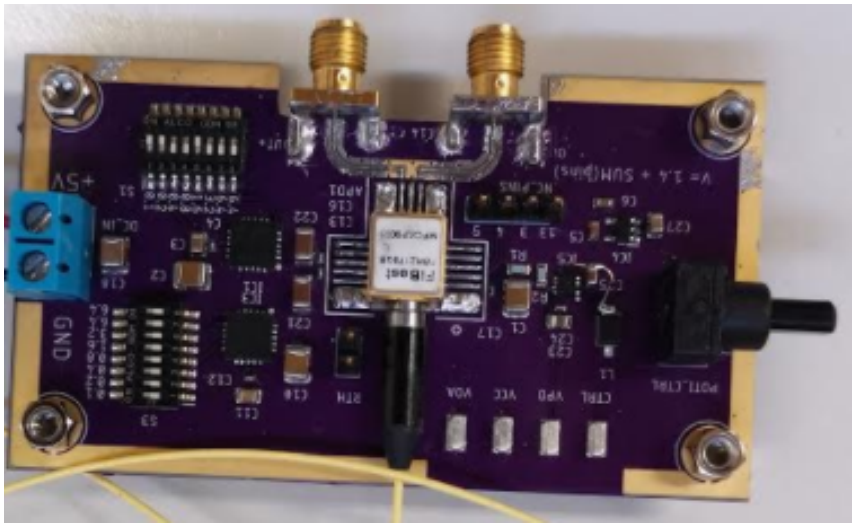

(a)

(b)

Figure 5.14: Final hardware of the optical receiver

5.3 Correction on the PCB

1. After the PCB arrived it was obvious that the footprint for the SMA connectors were not the correct ones. The problem was that the footprint of the SMA was too large that it will introduce reflexions on the ports, thus degrading the signal quality. To correct this error, the SMA pads were cutout and manual fixing is preformed to fit new SMA connectors.

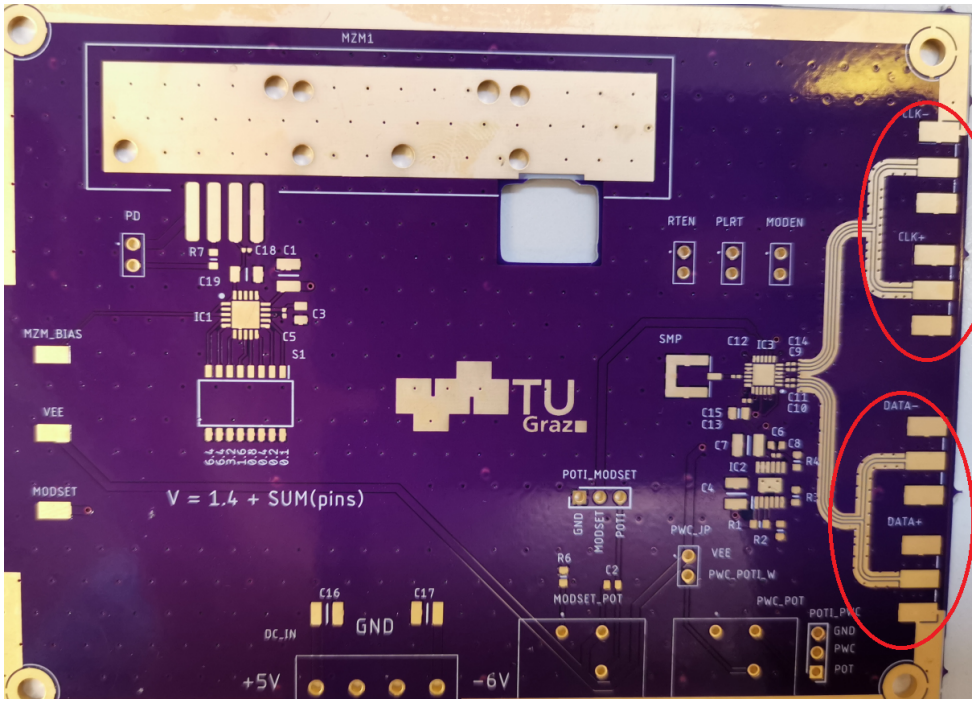

Figure 5.15: Correction of SMA Connectors

2. Another point was with the DC-DC converter in the optical receiver layout. Two input pins where not connected in the beginning, so the soldering of a jumper cable was necessary to fix this issue.

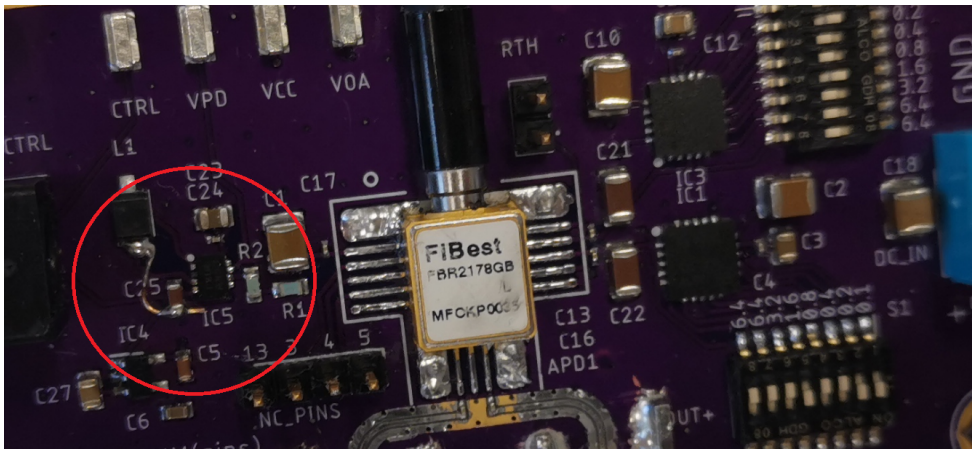

Figure 5.16: Soldering of a jumper

3. VIAs on the LDO and MZM driver chips were forgotten in the design phase of the transmitter PCB. Fortunately, they did not cause any problem later when testing the board.

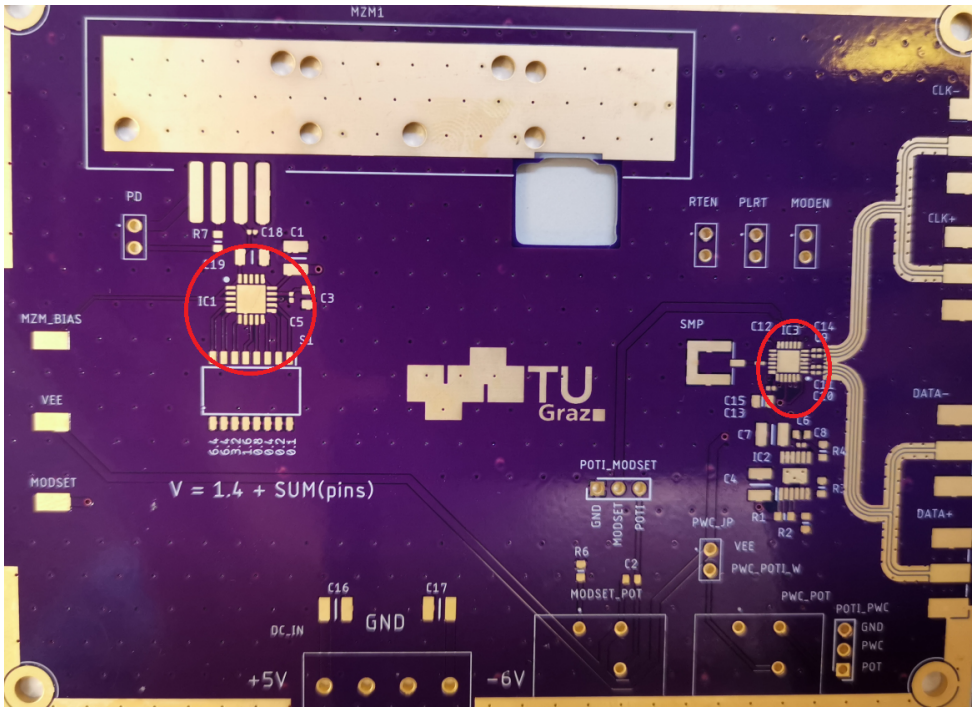

Figure 5.17: Forgot to place Vias

5.4 Measurements

Figure 5.18 shows the measurement setup for the optical system. The optical table and the collimator were only used in the last section for the free space scenario.

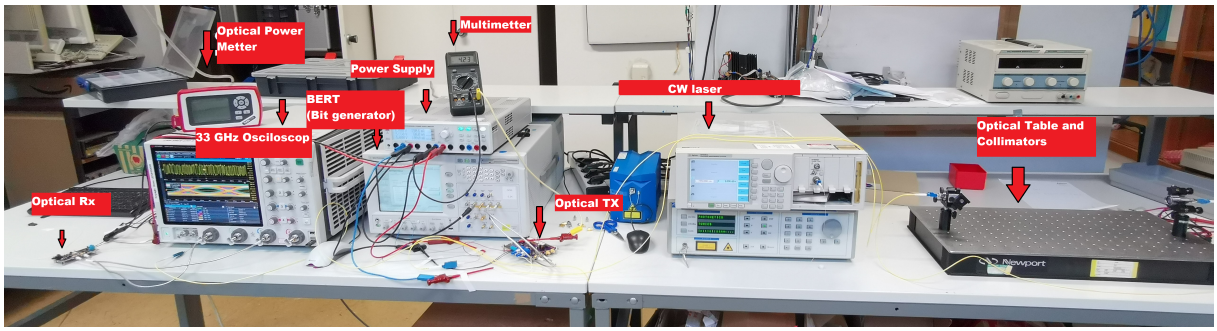

Figure 5.18: Measurements in the Optical Laboratory

5.4.1 MZM BIAS

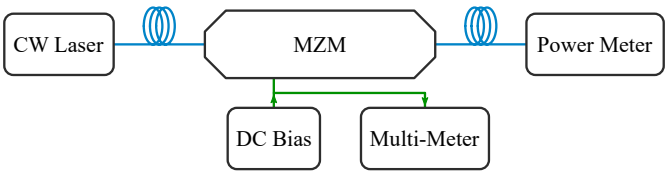

Figure 5.19: MZM Bias

The first measurement was with the bias of MZM. The measured bias voltage of MZM is to determine the DC bias point and the driving voltage. The results showed that the driving voltage is 2 V and the bias point is by 4.22 V. The measurement was done using a CW laser and monitoring the voltage with a multimeter. The voltage was increased and the optical output power of the MZM was observed. With this information it was possible to adjust the output of the driver so that the maximum efficiency is achieved. Figure 5.20 and Table 5.3 shows the bias voltage and optical output of MZM, and from there it is possible to determine the bias point (4.2 V) and the maximum driving voltage (2V).

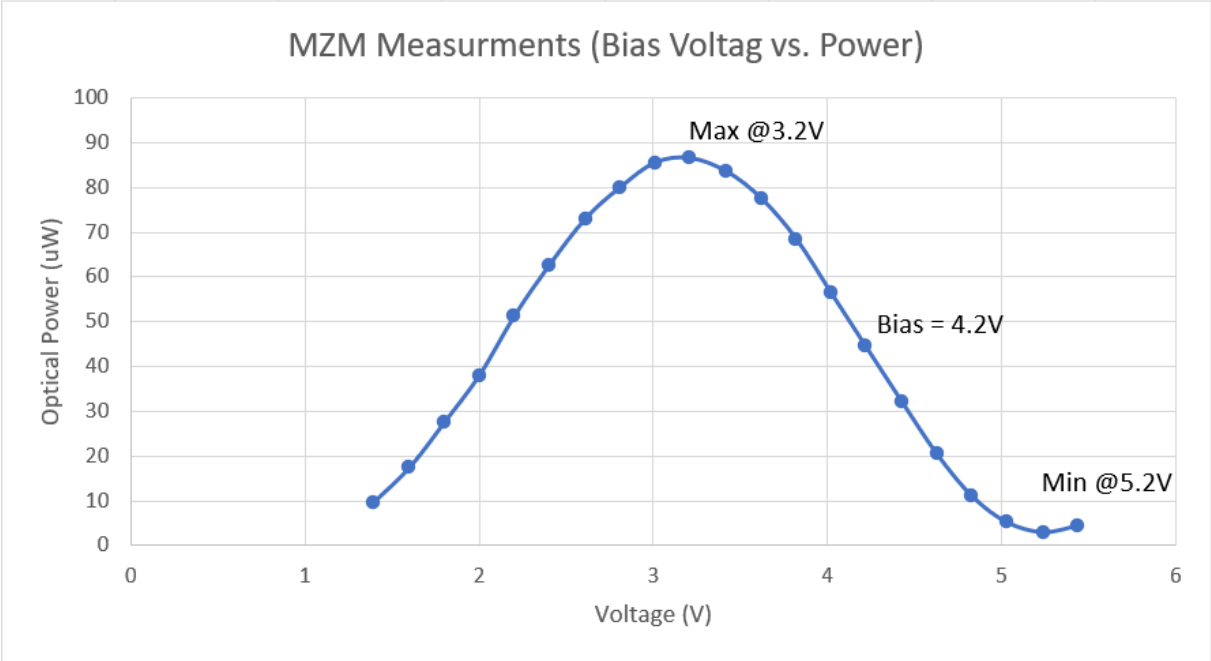

Figure 5.20: MZM Bias Voltage vs Power

Voltag (V)	Power (uW)	Voltag (V)	Power (uW)
1.39	9.5	3.62	77.5
1.6	17.48	3.82	68.5
1.8	27.55	4.02	56.5
2.2	51.2	4.22	44.5
2.4	62.5	4.43	32
2.61	73	4.63	20.4
2.81	80	4.83	11.05
3.01	85.5	5.03	5.2
3.21	86.5	5.24	2.93
3.42	83.5	5.44	4.42

Table 5.3: Bias Voltage vs Power

5.4.2 MZM Drive Voltage

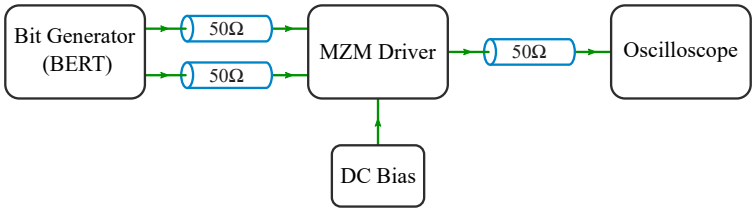

Figure 5.21: MZM driver schematic

The potentiometer is used to regulate the output voltage of the driver and set it up at 2Vpp at 10 Gbps. The eye diagram of the MZM driver is shown in Figure 5.22.

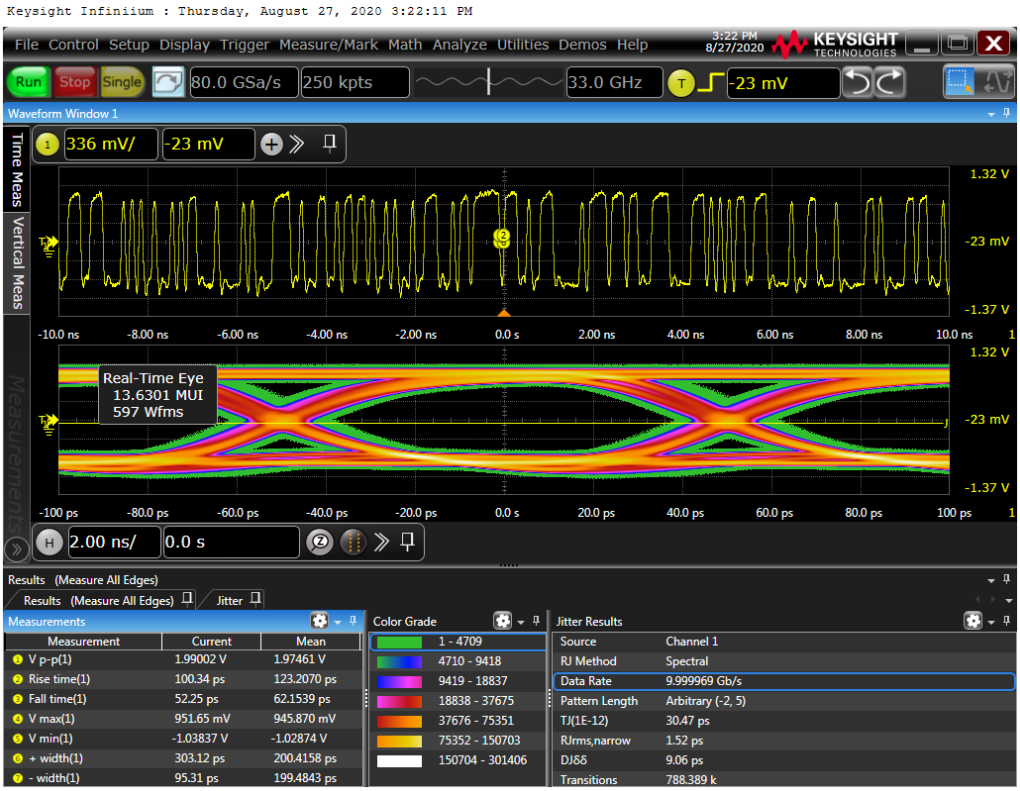

Figure 5.22: MZM driver 10 Gbps Eye Diagram

5.4.3 Eye Diagram

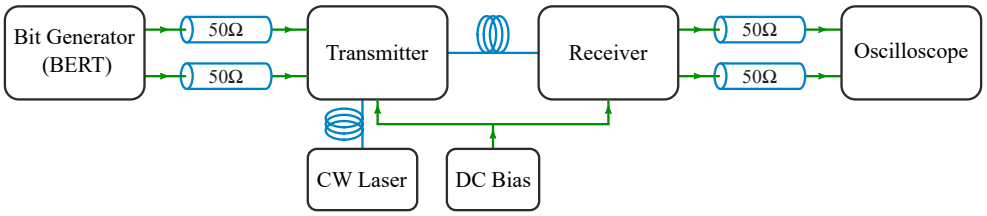

Figure 5.23: Optical Eye Diagram schematic

The eye diagram is used to get insights on signal quality, and it provides information on jitter. The eye diagram is a better alternative to BER analysis, as it can easily detect distortions and find the source of the problem. Figure 5.24 presents the optical eye diagram at 1 Gbps. It is to observe from the eye diagram, that it's a perfect eye with a very low jitter. Figure 5.25, 5.26 and 5.27 present the eye diagram from 3 Gbps till 8 Gbps.

Figure 5.24: Eye Diagram at 1 Gbps

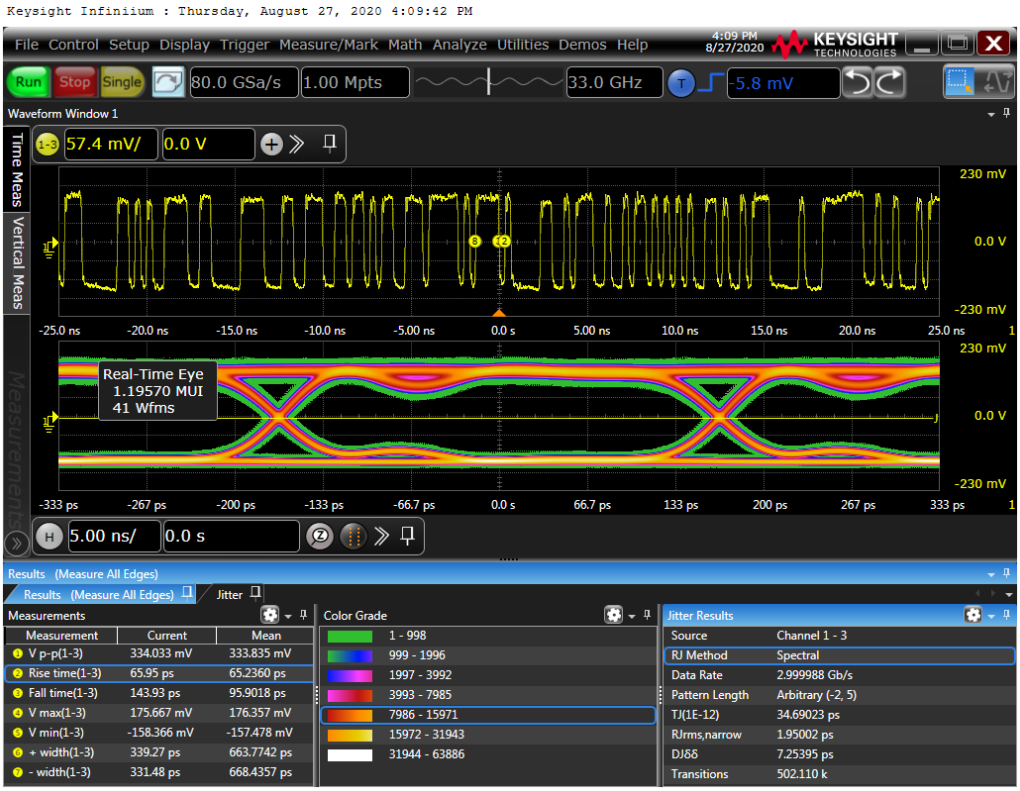

Figure 5.25: Eye Diagram at 3 Gbps

Figure 5.26: Eye Diagram at 5 Gbps

In Figure 5.27 it is to observe that by increasing data rate, the rise time reaches its limit. This is the reason that the eye looks elliptic and not rectangular as in Figure 5.26.

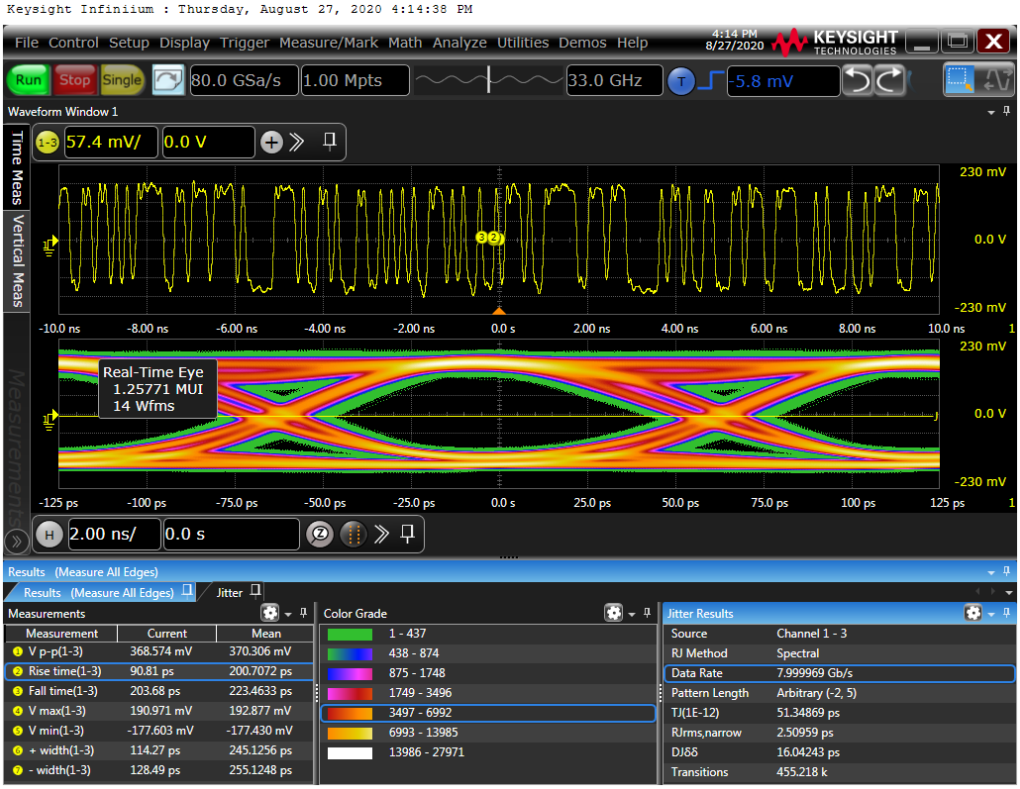

Figure 5.27: Eye Diagram at 8 Gbps

Figure 5.28 shows the eye diagram of 10 Gbps. This was the goal of this thesis. The eye is still open and the digital transmission is still valid.

Figure 5.28: Eye Diagram at 10 Gbps

Figure 5.29 shows the eye diagram at 12 Gbps and the eye is still open but is reaching its limit.

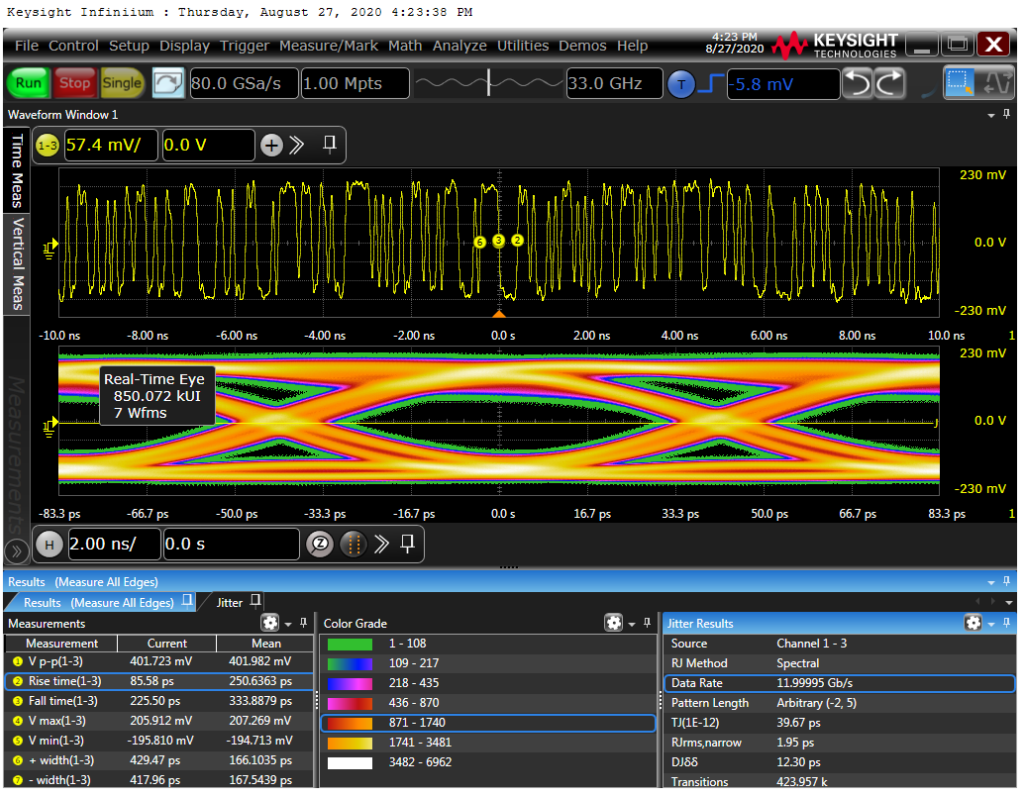

Figure 5.29: Eye Diagram at 12 Gbps

5.4.4 BER

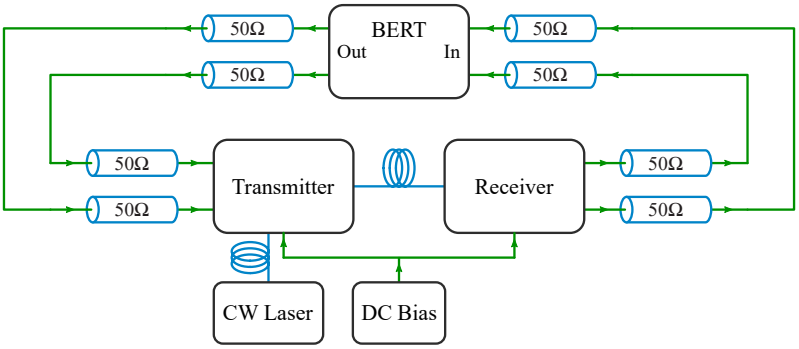

Figure 5.30: BERT Schematic

Since the BERT (Agilent Technologies N4906B) is connected directly with the the transmitter and receiver, it is difficult to measure the BER at short distance. Figure 5.31 shows the BER at 10 Gbps (which is 0).

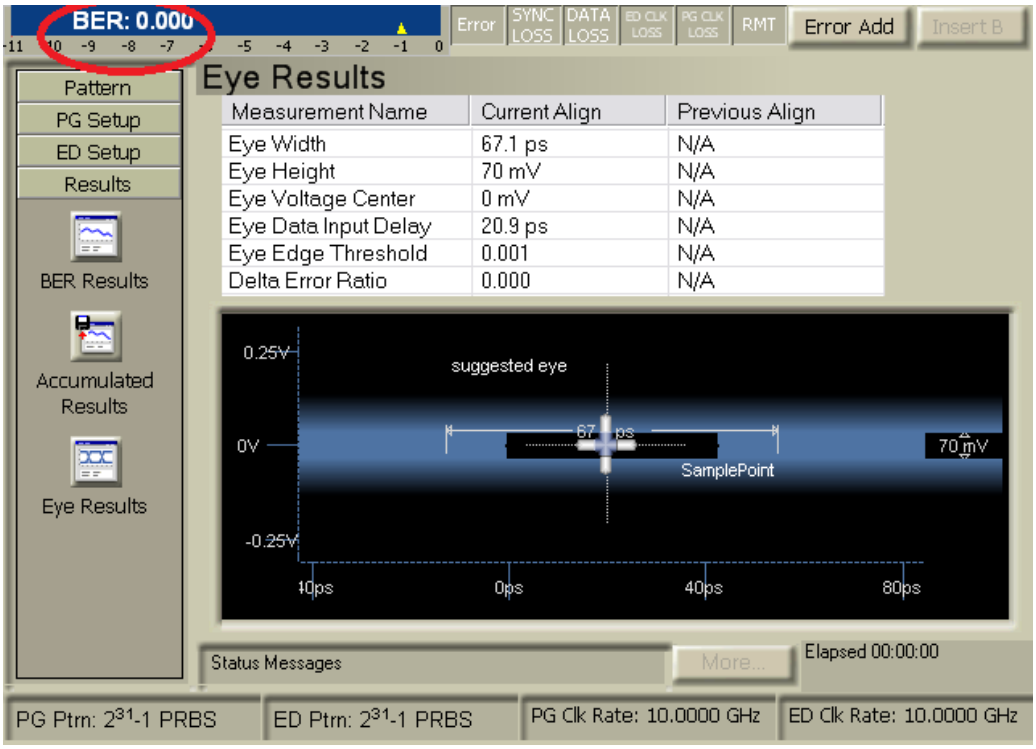

Figure 5.31: BER

5.4.5 Free Space Optics Demo

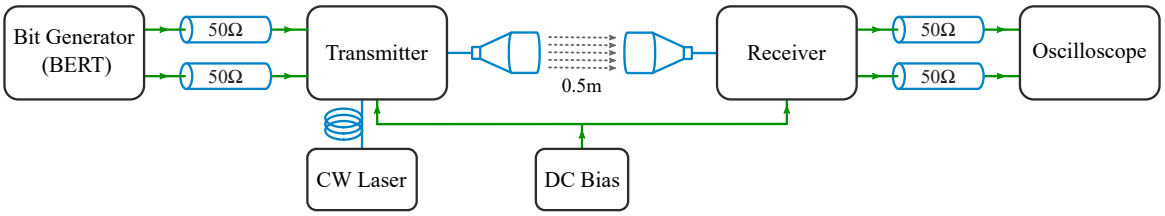

Figure 5.32: Demo schematic

The transmitter and receiver where tested in a demo setup in free space optic scenario using two collimators attached to an optical table. The work was done for a small distance, but this should be enough for demonstration to show that the hardware could be integrated into an FSO optical system.

Figure 5.33: Optical Collimators

Figure 5.34: FSO Demo Scenario at 10 Gbps

6. Conclusions

The aim of this thesis was the hardware implementation and verification of a 10Gbps Transceiver for Optical Wireless Communication at 1550 nm. The design of the optical system was successful and it worked even at higher data rate than 10 Gbps, but after 12 Gbps it starts to reach its limit. Furthermore, we introduced the PCB design of the optical system created with the software program Eagle, including the schematic and the layout for the board. After that, an introduction of the stack up of a grounded and differential coplanar waveguide was shown, which include the results of the matching parameters. The MZM driver can reach a data rate up to 10.7 Gbps, and for the power supply the positive and negative LDO regulators where chosen because of their low noise characteristics. For the optical receiver, an APD was used, and an integrated TIA that requires a supply voltage of 3.3 Volt. After the design was done some issues had to be corrected, like the problem with the SMA connectors and the DC-DC converters (see chapter 5), After solving these issues we were able to test the System. Using a 33 Gbps Oscilloscope it was possible to show the perfect eye diagram with a very low jitter for 1 Gbps and continued like this until we reached 12 Gbps. The BER measurements and a demo setup of free space optic scenario using two collimator attached in an optical table in short distance where successfully analyzed. The goal of development and analysis of an FSO system has been achieved and the results showed that the hardware can be integrated into an FSO system and can be used for further projects.

For the future, additional improvements can be done on this work, e.g., implementing another transceiver for bi-directional communication, and building a housing for the system for ease of use. Furthermore, because of the analog nature of the system, one can use it to convert optical signals into RF, e.g., measuring optical signals with RF oscilloscope. Additional future works can include: parallel transmission (doubling the data rate), optic-MIMO (Multiple-Input-Multiple-Output), implementation of IQ-based (In-phase and Quadrature-phase) modulation by using multiple MZMs, etc. In general, future works with multiple optical transceivers can be endless.

Bibliography

[1] O. Bouchet, H. Sizun, C. Boisrobert, F. de Fornel, and P. Favennec, *Free-Space Optics: Propagation and Communication*, ser. ISTE. Wiley, 2010.

[2] E. Sackinger, *Broadband Circuits for Optical Fiber Communication*. 2005 byJohn Wiley, 1959.

[3] X. Fu, G. Chen, T. Tang, Y. Zhao, P. Wang, and Y. Zhang, "Research and simulation of ppm modulation and demodulation system on spatial wireless optical communication," in *2010 Symposium on Photonics and Optoelectronics*. IEEE Conference Publications, 2010, pp. 1–5.

[4] H. Kaushal, V. Jain, and S. Kar, *Free Space Optical Communication*, ser. Optical Networks. Springer India, 2017.

[5] R. I. S. M. S. Z. Ramirez Iniguez, *Optical Wireless Communications: Ir For Wireless Connectivity*. TAYLOR and FRANCIS GROUP LLC, 2008.

[6] C. J. R. Capela, "Protocol of communications for vorsat satellite," Master's thesis, Universidade do Porto, Porto, 4 2012.

[7] D. A. Raj and A. Majumdar, "Historical perspective of free space optical communications: from the early dates to today's developments," *IET Communications*, vol. 13, pp. 2405–2419, 08 2019.

[8] A. G. Alkholidi and K. S. Altowij, "Free space optical communications — theory and practices," in *Contemporary Issues in Wireless Communications*, M. Khatib, Ed. Rijeka: IntechOpen, 2014, ch. 5. [Online]. Available: https://doi.org/10.5772/58884

[9] A. A. B. Raj, *Free space optical communication : system design, modeling, characterization and dealing with turbulence*. Wiley, 2016.

[10] E. Leitgeb, T. Plank, P. Pezzei, D. Kraus, and J. Poliak, "Integration of fso in local area networks - combination of optical wireless with wlan and dvb-t for last mile internet connections," in *2014 19th European Conference on Networks and Optical Communications - (NOC)*, 2014, pp. 120–125.

[11] F. Nadeem, V. Kvicera, M. S. Awan, E. Leitgeb, S. S. Muhammad, and G. Kandus, "Weather effects on hybrid fso/rf communication link," *IEEE Journal on Selected Areas in Communications*, vol. 27, no. 9, pp. 1687–1697, 2009.

[12] P. Nikolas, "Characterization of signal fluctuations in optical communications with intensity modulation and direct detection through the turbulent atmospheric channel," Master's thesis, Universidade de Valencia, Weiling, november 2005.

[13] H. G. Abreha, "Analysis of high-speed transmitter path diversity scheme in a dwdm free-space optical communications test link," Master's thesis, German,Münich, The address of the publisher, 1 2014.

[14] W. R. S. Ghassemlooy, Z. Popoola, *Optical Wireless Communications: System and Channel Modelling with MATLAB.* CRC Press, 2013.

[15] G. A. Mahdiraji and E. Zahedi, "Comparison of selected digital modulation schemes (ook, ppm and dpim) for wireless optical communications," in *2006 4th Student Conference on Research and Development.* IEEE Conference Publications, 2006, pp. 5–10.

[16] W. Gappmair, S. Hranilovic, and E. Leitgeb, "Performance of ppm on terrestrial fso links with turbulence and pointing errors," *IEEE Communications Letters*, vol. 14, no. 5, pp. 468–470, 2010.

[17] B. Hillbrand, "Erweiterung des fso-kanalmodells für mehrere atmosphärenschichten und implementierung der era-15 daten," Master's thesis, Institut für Breitbandkommunikation Technische Universität Graz, Graz, 1 2010.

[18] A. Uzbekov, "Feasibility study of free-space optical links for micro- and nano- satellites," Master's thesis, Moscow Institute of Physics and Technology, Moscow, 1 2015.

[19] Z. Ghassemlooy, W. O. Popoola, and E. Leitgeb, "Free-space optical communication using subearrier modulation in gamma-gamma atmospheric turbulence," in *2007 9th International Conference on Transparent Optical Networks*, vol. 3, 2007, pp. 156–160.

[20] T. Enduroat, "Link budget,innospacetool unit 10 complementary material," *InnoSpaceTool*, vol. 10, p. 5, 1 2020.

[21] T. Plank, M. Czaputa, E. Leitgeb, S. S. Muhammad, N. Djaja, B. Hillbrand, P. Mandl, and M. Schönhuber, "Wavelength selection on fso-links," in *Proceedings of the 5th European Conference on Antennas and Propagation (EUCAP)*, 2011, pp. 2508–2512.

[22] Analog Device, "–20v, 500ma, ultralow noise, ultrahigh psrr negative linear regulator," Accessed on 2020-Jul-01. [Online]. Available: https://https://www.mouser.at/datasheet/2/609/LT3094-1504100.pdf

[23] MAXIM, "Max3941, 10gbps eam driver with integrated bias network," Accessed on 2020-Jul-01. [Online]. Available: https://datasheets.maximintegrated.com/en/ds/MAX3941.pdf

A. Equipments

A.1 Equipment List

Device	Manufacturer and properties
Power Supply	HAMEG Instruments Programmable Power Supply HMP2030
Optical Powermeter	Thorlabs PM100D
Digital Multimeter	Digital Multimeter TDM 600 600V CAT II
CW Laser	Agilent 8164A Lightwave Measurement System
BERT	Agilent Technologies N4906B
Optical table	Newport 544 637
Fiber collimator	Thorlabs F810FC-1550
33 GHz Oscilloscope	KEYSIGHT DSA-V 334A

Table A.1: Equipment

A.2 Data Sheets

The data sheet of the MZM and APD are found in the next pages.

LN MODULATORS

10Gbit/s Low Drive Voltage LN Intensity Modulator (Single Electrode Model)

Specifications

Model		T-MXH1.5-10PD-ADC-LV (Zero Chirp)
Operating Wavelength		1.55μm
Insertion Loss		≦6.0dB
Driving Voltage @1kHz		≦3.0V
Driving Voltage(Vπ)@10Gbps		≦3.0V(Typ.2.4V)
Optical Bandwidth*1		≧8GHz
ON/OFF Extinction Ratio		≧20dB
Polarization Extinction Ratio		≧20dB
Optical Return Loss		≧30dB
Chirp Parameter α(Typ.)		-0.2～0.2
Maximum Input Power*2		20mW
Optical Fiber	Input	0.9mmΦPMF FC Connector
	Output	0.9mmΦPMF SC Connector
Electrical Connector		GPO Connector
Fiber Lead Length		≧0.7m
Operating Temperature		0℃～70℃
Polarizer		Included

PD Characteristics	
Monitor PD Sensitivity	0.01～0.40 mA/mW
Monitor PD Extinction Ratio	≧8dB

*1: 3dBdown(1GHz reference)
*2: Input polarization must be aligned to the slow axis of polarization maintained fiber before the maximum input power is inserted.

Ordering Information

T.MXH1.5-10PD-ADC-LV-04-004

＊: Standard optical connector is shown in the specification.
If you need the different connector(s), please let us know.

＊: The polarization state of the PMF is slow axis aligned.

Package size(Hermetically-sealed)

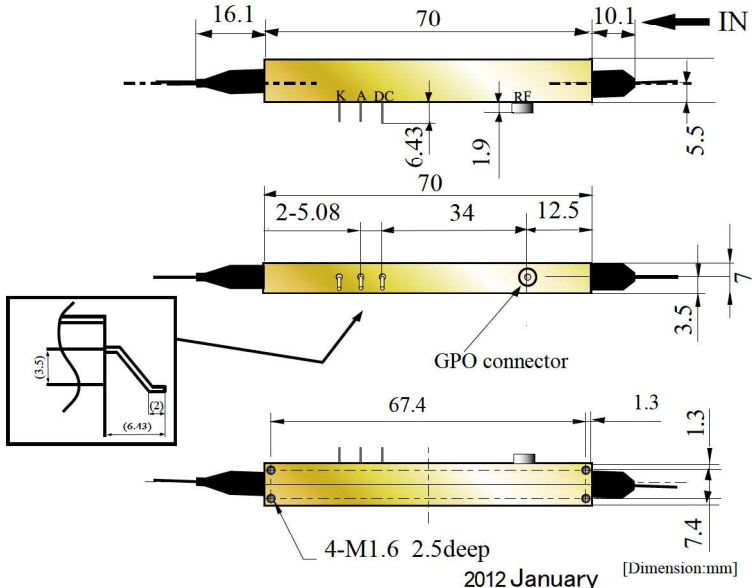

[Dimension:mm]

2012 January
*Specifications subject to change without any notice.

Manufactured by :
SUMITOMO OSAKA CEMENT CO.,LTD.
OPTOELECTRONICS BUSINESS DIVISION

Eudyna (Sumitomo Electric) APD

Table: Part Numbers	
Optical Connector Type	Supplier Part Number
LC-BTW	ERA1459GT600L
MU	ERA1459GT600M

Pinning

No	Symbol	Function
1	GND	Case Ground
2	V_{PD}	PD Supply Voltage
3	NC	No connection
4	NC	No connection
5	NC	No connection
6	GND	Case Ground
7	GND	Case Ground
8	OUT_N	Negative Output
9	GND	Case Ground
10	OUT_P	Positive Output
11	GND	Case Ground
12	GND	Case Ground
13	NC	No connection
14	V_{CC}	TIA Supply Voltage
15	VOA	VOA control voltage
16	R_{th}	Thermistor
17	GND	Case Ground

Operating Conditions						
Item	*Parameter*	*Symbol*	*Condition*	*Min*	*Max*	*Unit*
1	Operating case temperature range	T_{case}	Long Term	-5	80	°C
			Short Term (see note 1)	-5	85	°C
2	Operating wavelength range	λ		1528	1569	nm
3	Average optical input power range with VOA	P_{opt}	*VOA active*	-22	8	dBm
4	V_{PD} *for* $M = 3$	V_{M3}	P_{opt} = -5dBm, VOA inactive	V_{M3}		V
5	V_{PD} for $M = M_{opt}$	V_{Mopt}	P_{opt} = -27dBm VOA inactive	V_{Mopt}		V
6	TIA supply voltage	V_{CC}		+3.2	+3.4	V
7	Extinction Ratio of input signal	*ER*	see note 4	12	-	dB
8	Output load termination to GND (OUT_N, OUT_P)	R_{Load}	via external DC block	50		Ω

*)Values provided by Eudyna for each device, V_{M3} and V_{Mopt} are voltages measured direct on package pin #2, respectively.

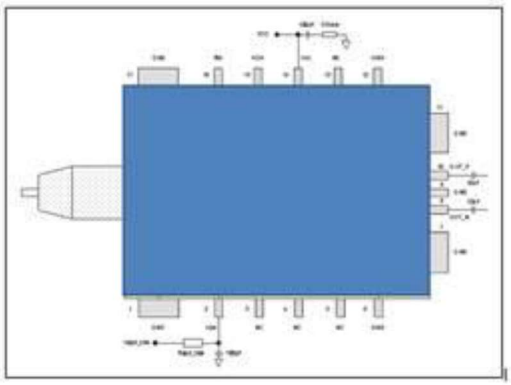

End of life shall have occurred when any of the specifications given in this section are exceeded.

Table: EOL Optical and Electrical Characteristics

Item	*Parameter*	*Symbol*	*Condition*		*Min*	*Max*	*Unit*
1	Sensitivity	P_{sens}	10.7 Gbs, NRZ, PRBS 2^{31}-1, BER = 10^{-12}, decision threshold at 50%, $M = M_{opt}$	T_{case}= 25°C	-	-26.0	dBm
				T_{case}= -5 to 80°C	-	-25.0	
2	Overload	P_{overl}	10.7 Gbs, NRZ, PRBS 2^{31}-1, BER = 10^{-12}, decision threshold at 50% $M = 3$		-4	-	dBm
3	Overload	P_{overl_voa}	10.7 Gbs, NRZ, PRBS 2^{31}-1, BER = 10^{-12}, decision threshold at 50% $M = 3$ *Att = 12dB*		+8.0	-	dBm
4	Maximum AC transimpedance (differential)	Z_{tmax}			5000	10000	Ω
5	Minimum AC transimpedance (differential)	Z_{tmin}			-	300	Ω
6	3dB cut-off frequency of transfer function S_{21}	f_{-3dB}			6.5	-	GHz
7	Low frequency cut off	f_{-3dB_L}	10µF DC-block at output		5	100	kHz
8	Differential output reflection coefficient	$\lvert S_{22}\rvert_{diff}$	100MHz through 6.0GHz		-	-7	dB
			6.0GHz through 10GHz		-	-6	dB
9	Input noise current	I_{noise}			-	1.7	μA_{RMS}
10	Output swing (differential)	V_{out_ac}	P_{opt} = -5dBm, $M = 3$		210	430	mV
11	Output DC offset	V_{offset}	$OUT\_P_{DC} - OUT\_N_{DC}$		-50	50	mV
12	Photo diode DC responsivity	R	λ = 1550nm, Polarization scrambled, $M = 1$ see note 5		0.7	1.05	A/W
13	Change of photo diode DC responsivity due to polarization	ΔR_{pol}	T_{case} = 25°C, 0dB ≤ *Att* ≤ 5dB $M = 1$ see note 6		-	0.4	dB

Table: EOL Optical and Electrical Characteristics						
Item	*Parameter*	*Symbol*	*Condition*	*Min*	*Max*	*Unit*
			5dB ≤ *Att* ≤ 20dB	-	0.7	dB
14	Photo diode dark current	I_{dark}	T_{case} = 25°C M = 3	-	50	nA
			T_{case} = 25°C $M = M_{opt}$	-	220	nA
			T_{case} = 80°C $M = M_{opt}$	-	2000	nA
15	TIA supply current	*Icc*			83	mA
16	Power dissipation	P_{dis}	V_{CC} = Max, full temperature range *Att* = 20dB	-	450	mW
17	*k* Factor	*k*	T_{case} = 25°C	1.0		-
18	APD breakdown voltage	V_{break}	T_{case} = 25°C	24	34	V
19	Aging of $M = f(V_{PD})$	ΔV_{PD}		-7.0	+7.0	%
20	Temperature coefficient of V_{APD}	γ	$\gamma = dV_{break}/dT_{case}$	30	70	mV/K
21	Thermistor Resistance	*Rth*	T_{case} = 25°C	9.5	10.5	kΩ
22	Thermistor B-Constant	*B*		3800	4000	K
23	Thermistor aging	ΔR_{th}		-2	2	%
24	VOA control voltage	V_{att}	*Att* = 20dB	-	5.0	V
25	VOA control power	P_{att}		0	160	mW
26	VOA attenuation range	*Att*		0.0	20.0	dB
27	maximum VOA attenuation slope	$max\ dAtt/dV_{voa}$	T_{case} = 25°C *Att* = [0 .. 20]dB	8.0	16.5	dB/V
28	VOA attenuation slope at 20dB	$dAtt/dV_{voa\|20dB}$	T_{case} = 25°C *Att* = 20dB	3.0	-	dB/V
29	VOA attenuation rise time (10%-90%)	t_{Att_rise}	V_{att} changed from 0V to V_{att} (*Att* = 20dB) V_{att} rise time < 1ms	-	5	ms
30	VOA attenuation fall time (90%-10%)	t_{Att_fall}	V_{att} changed from V_{att} (*Att* = 20dB) to 0V V_{att} fall time < 1ms	-	15	ms
31	Change of *Att* with temperature	ΔAtt_{ϑ}	*Patt = const.*	-	2	dB
32	Change of *Att* with wavelength	ΔAtt_{λ}	*Patt = const.*	-	0.7	dB
33	Change of *Att* due to aging	ΔAtt_{aging}	*Patt = const.*	-	0.5	dB

B. Optical Transmitter Board

B.1 Optical Transmitter

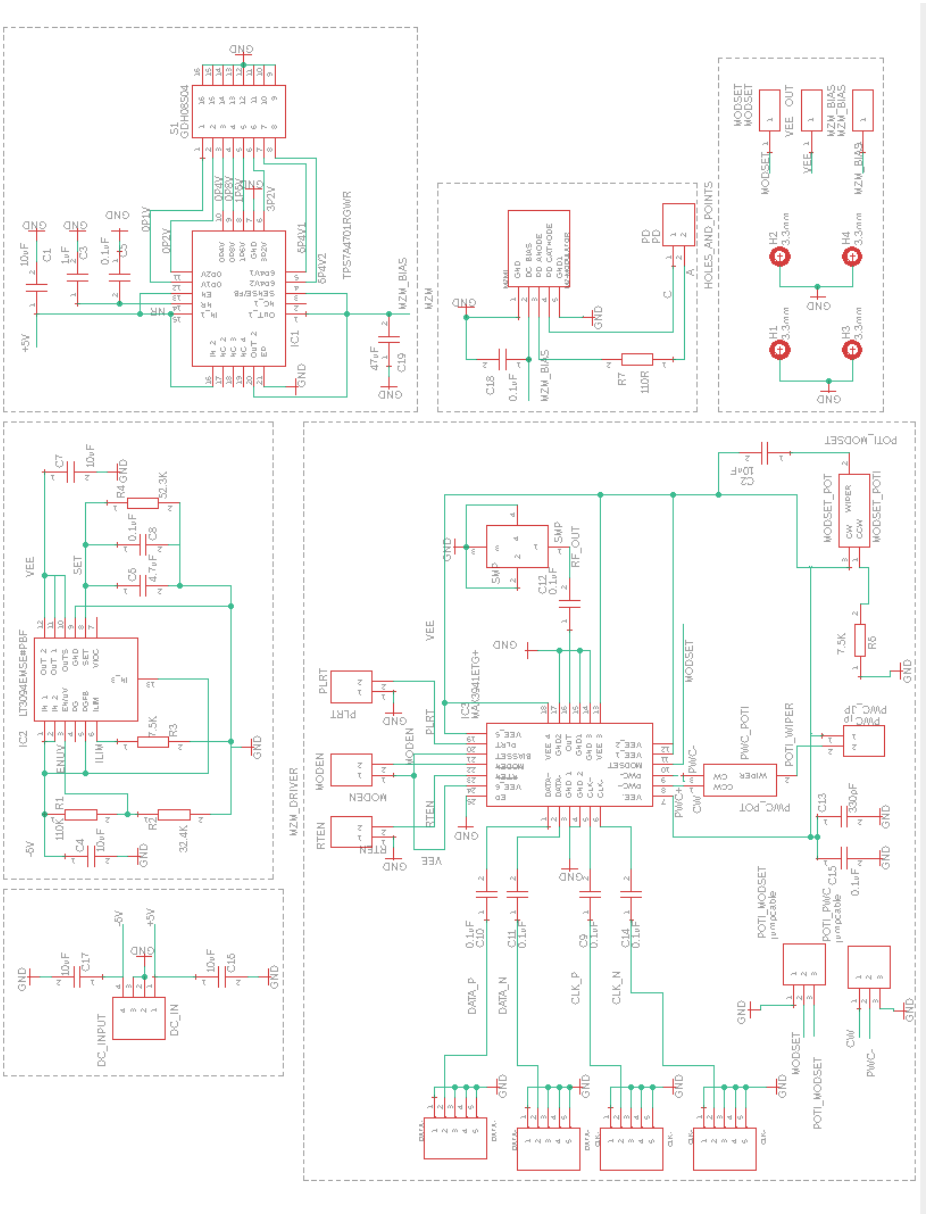

Figure B.1: PCB Transmitter Schematic 1

B.2 Top Plane

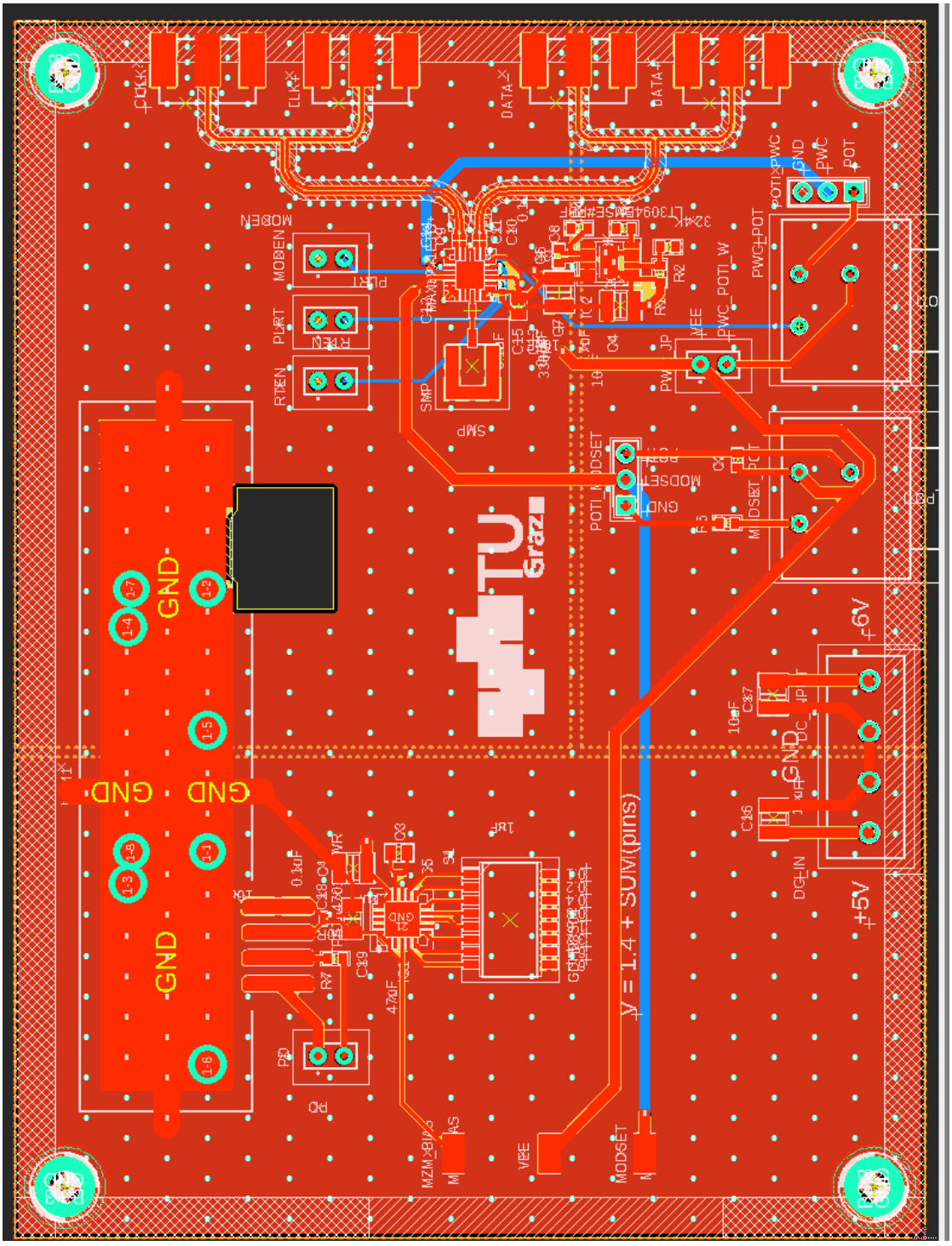

Figure B.2: Top Plane Board

B.3 Power Plane

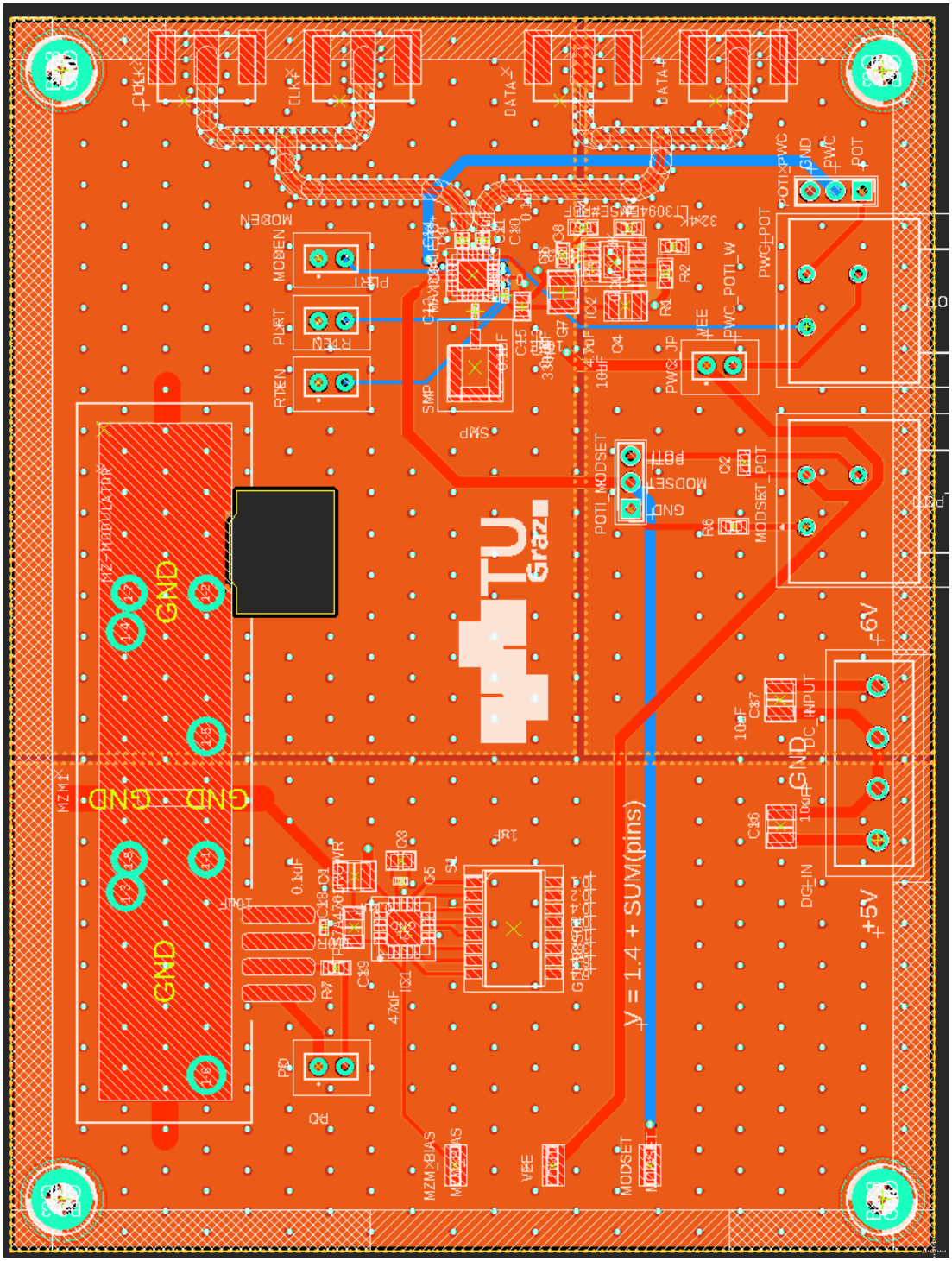

Figure B.3: Power Plane Board

B.4 GND Plane

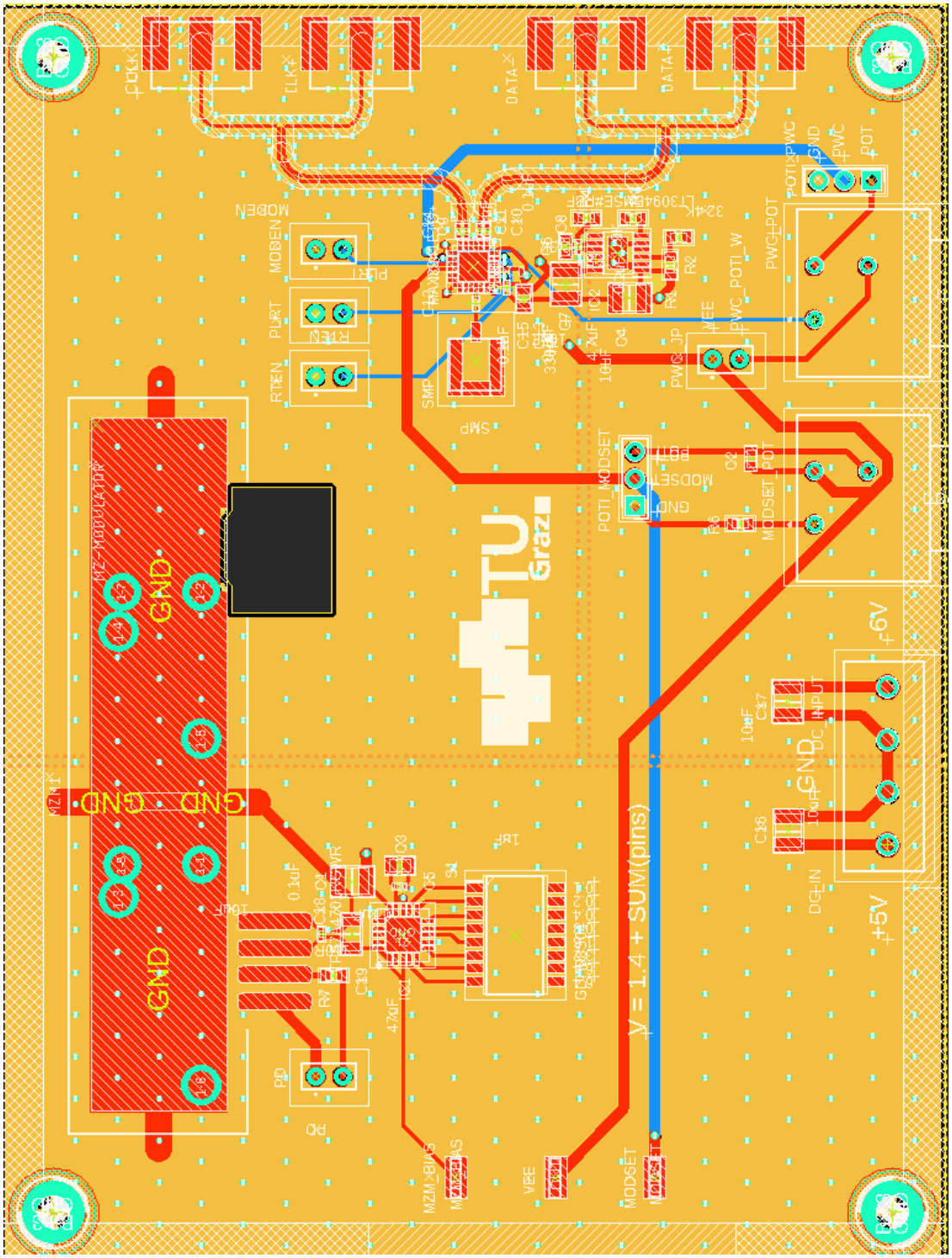

Figure B.4: GND Plane Board

B.5 Bottom Plane

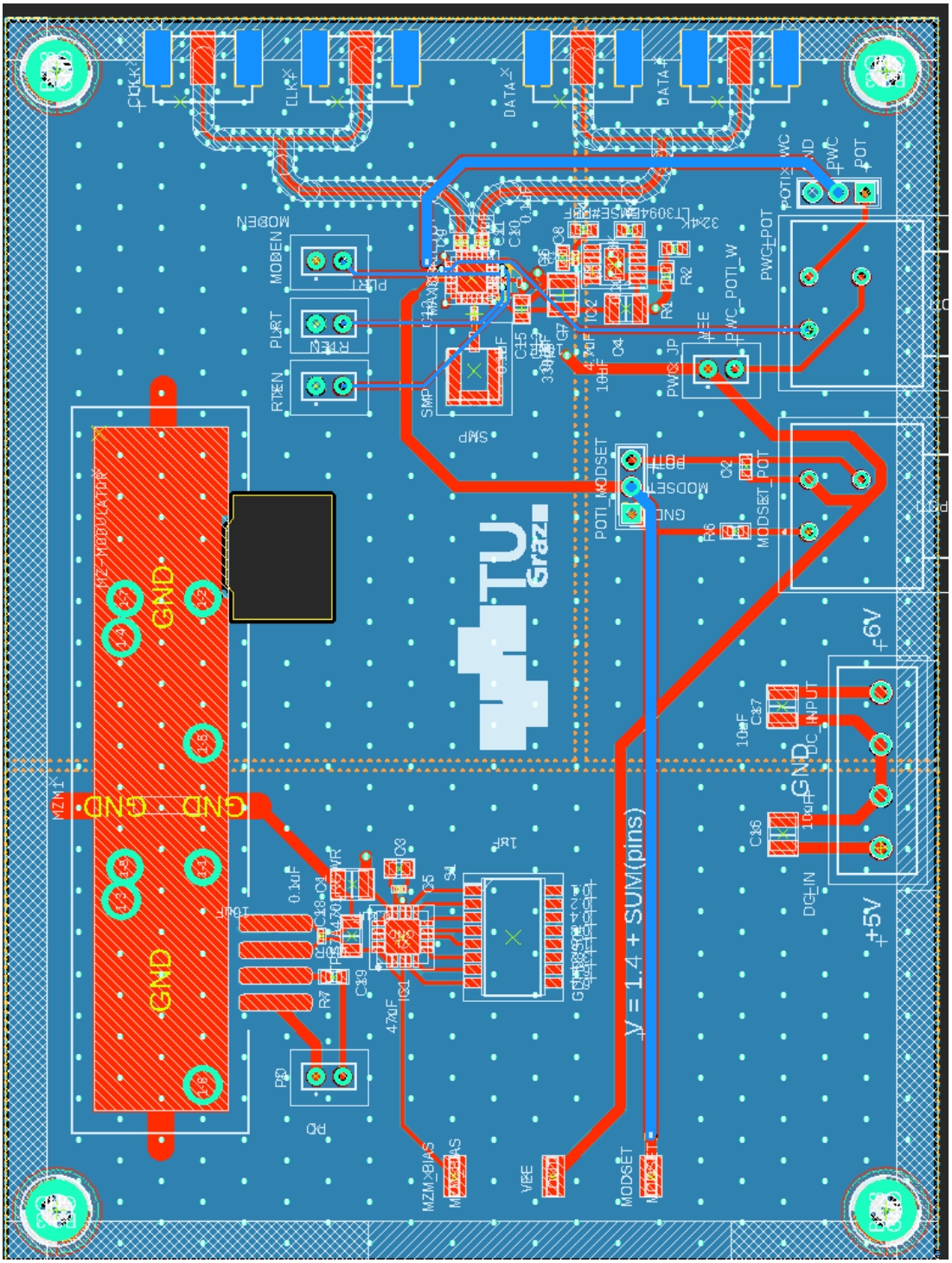

Figure B.5: Bottom Plane Board

C. Optical Receiver Board

C.1 Optical Receiver

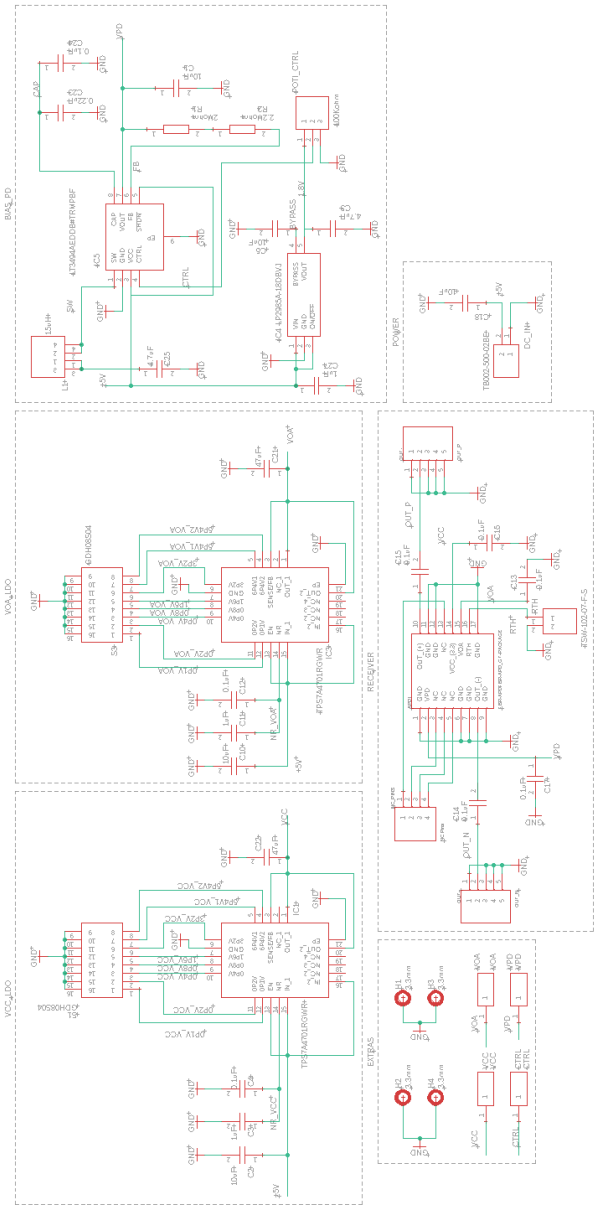

Figure C.1: Optical Receiver Schematic 1

C.2 Top Plane

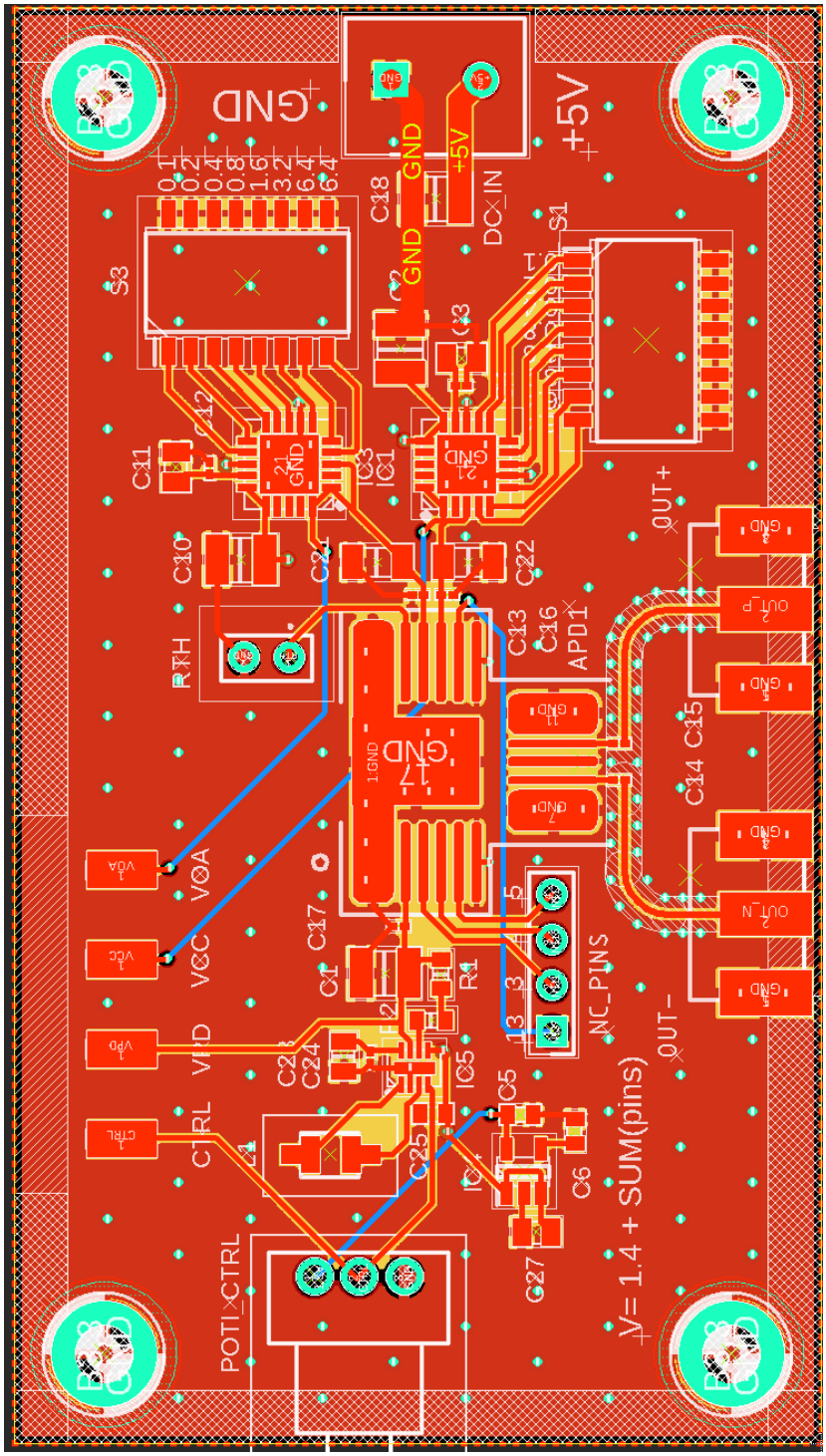

Figure C.2: Top Plane Board

C.3 GND Plane

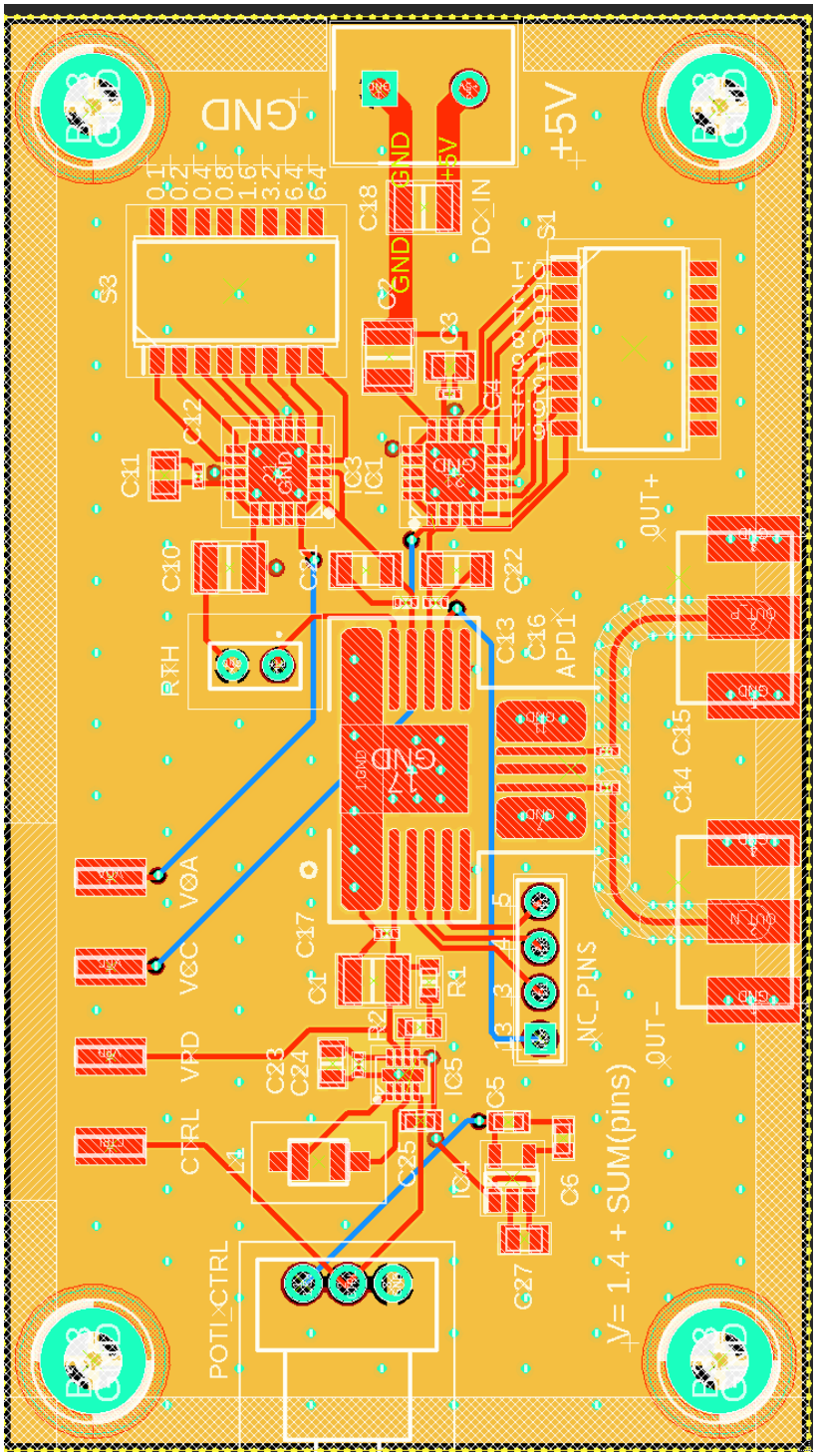

Figure C.3: GND Plane Board

C.4 Power Plane

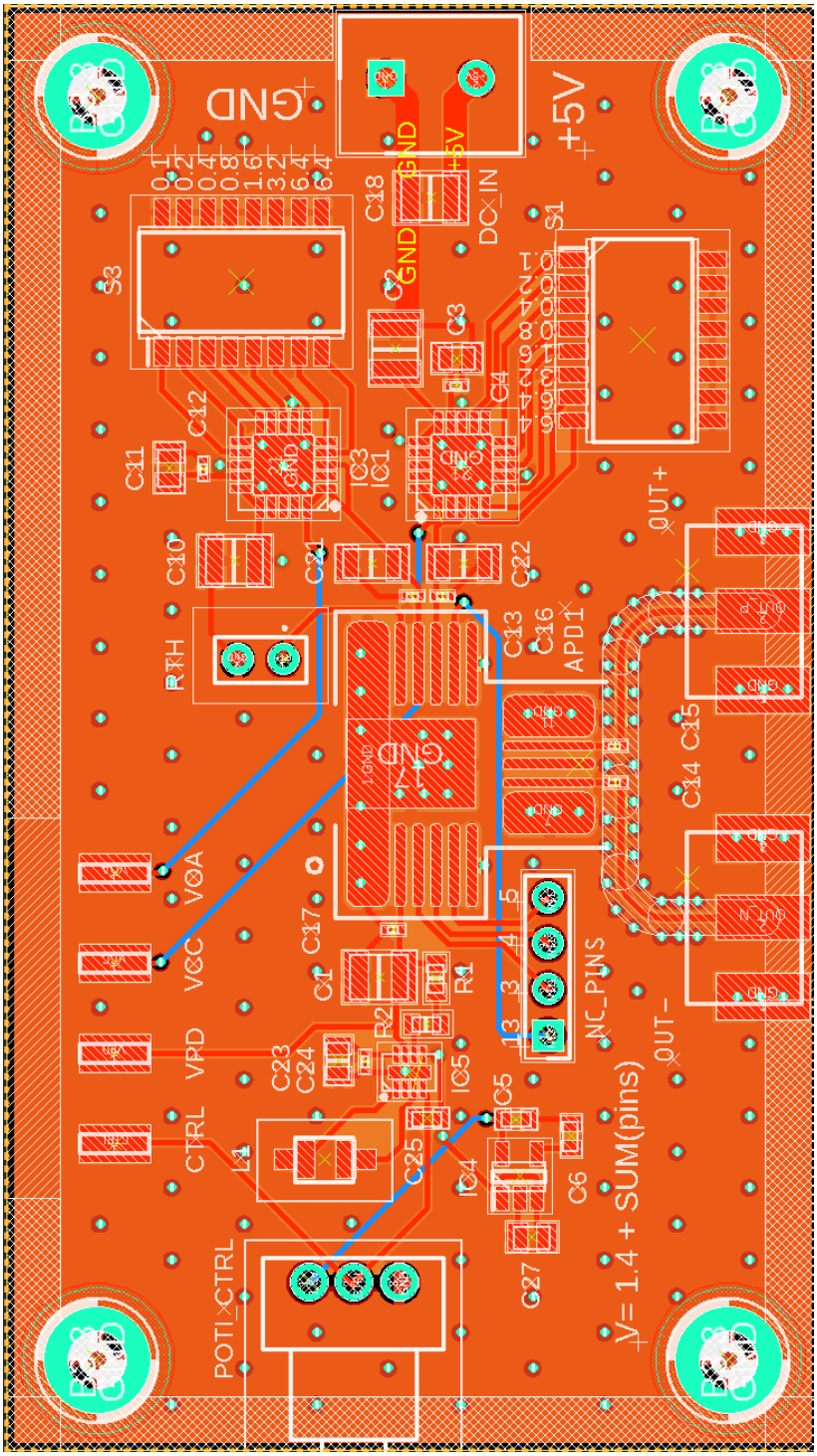

Figure C.4: Power Plane Board

C.5 Bottom Plane

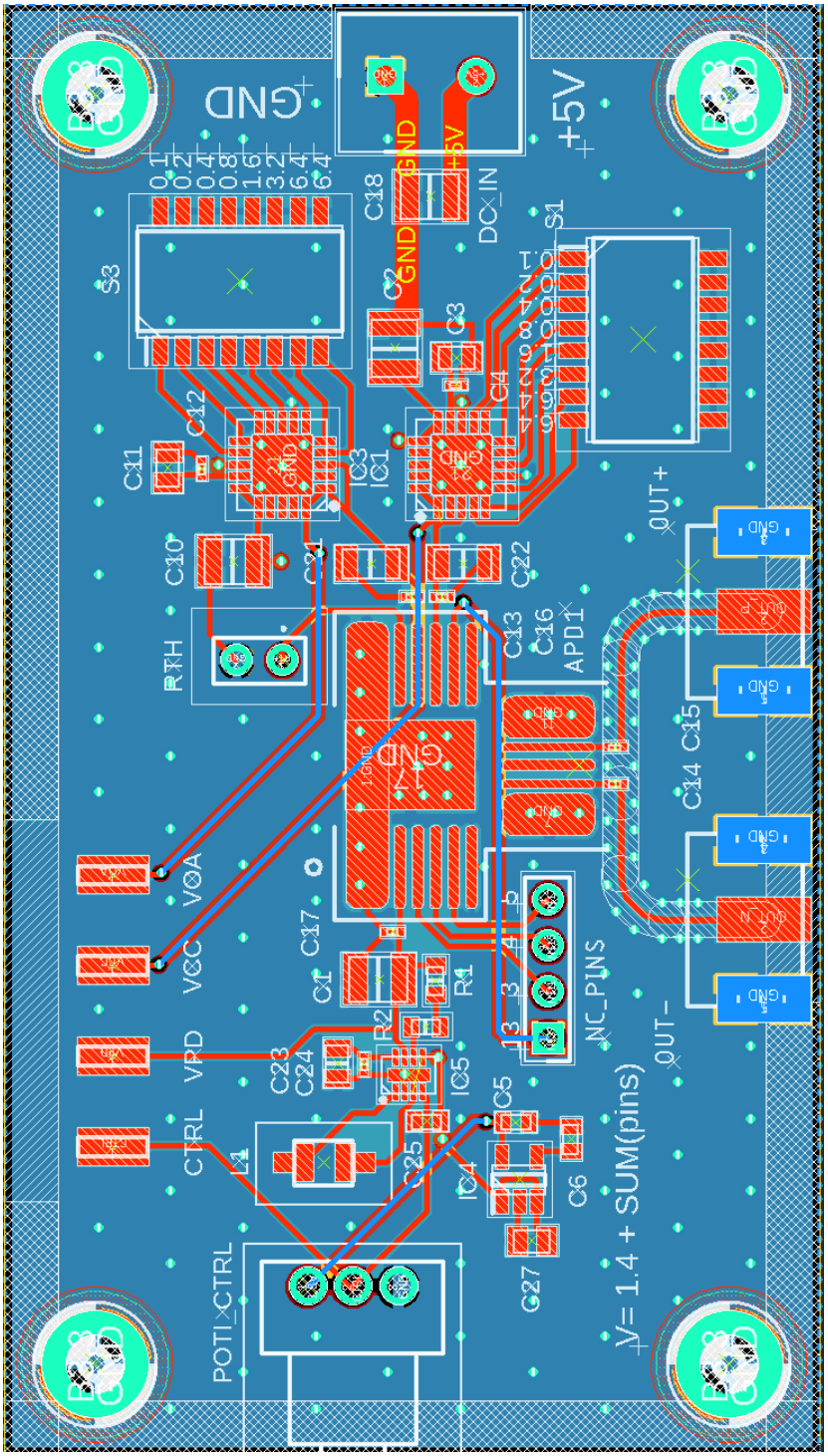

Figure C.5: Bottom Plane Board